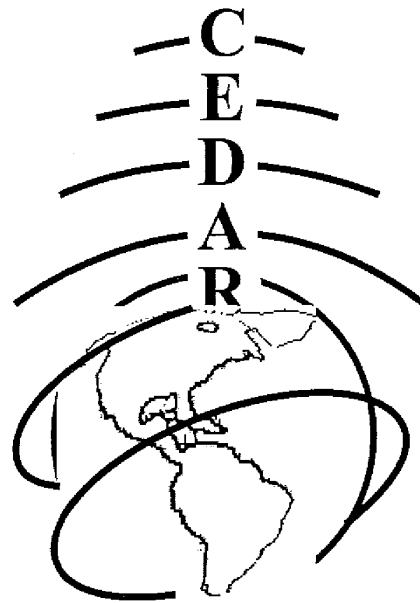




EDAR-GEM Joint Workshop

Santa Fe, New Mexico
June 19 - June 24, 2016



CEDAR IT Poster Session Booklet
Tuesday, June 21, 2016



Table of Contents

Equatorial Thermosphere or Ionosphere

EQIT-01	Kassamba Abdel Aziz Diaby, Estimating equatorial daytime vertical ExB drift velocities from magnetic field variations.....	1
EQIT-02	Jonathon Smith, Global Distribution and Characteristics of Equatorial Plasma Bubbles.....	1
EQIT-03	Matthew Young, Parametric Wave Growth in a Hybrid PIC/Fluid Simulation of the Equatorial E Region	1
EQIT-04	Tzu-Wei Fang, Equatorial-PRIMO (Problems Related to Ionospheric Models and Observations)	2
EQIT-05	Tzu-Wei Fang, Quantifying the sources of ionospheric Day-to-day variability ...	2
EQIT-06	Jiahao Zhong, Long-duration depletion in the topside ionospheric total electron content during the recovery phase of the March 2015 strong storm	3
EQIT-07	Qingyu Zhu, Simulations of vertical ion-drag effect on neutral winds and compositions at low and middle latitudes	3
EQIT-08	Arthur D. Richmond, What drives the electrodynamics of the low-latitude evening ionosphere?	4
EQIT-09	Jong-Min Choi, Periodicity in the occurrence of equatorial plasma bubbles	4
EQIT-10	Fasil Tesema Kebede, Thermospheric wind and temperature measurements using Fabry-Perot Interferometers (FPI) at equatorial region of Ethiopia.	4
EQIT-11	Daniel J. Fisher, Stormtime effects in the thermospheric neutral winds and temperatures over Brazil	5
EQIT-12	Pablo Reyes, Probing the equatorial ionospheric valley region fluctuations with Jicamarca ISR and VIPIR ionosonde	5
EQIT-13	Dustin A. Hickey, Airglow observations of the ionosphere from three imagers in South America	5
EQIT-14	Sovit Khadka, Contribution of Neutral Wind and Electrojet to the Structural Dynamics of Equatorial Ionization Anomaly	6

Irregularities of Ionosphere or Atmosphere

IRRI-01	Victoriya V. Forsythe, Asymmetries in the phase velocity of the E-region plasma irregularities at high southern latitudes	6
IRRI-02	Bea Gallardo-Lacourt, Influence of auroral streamers on rapid evolution of SAPS flows	6
IRRI-03	Leslie J Lamarche, Asymmetry in plasma irregularity growth near large-scale gradient reversals	7

IRRI-04	Tae-Yong Yang, First report of the afternoon E-region plasma density irregularities in middle latitude	7
IRRI-05	Brian Breitsch, Adaptive-Mesh Imaging of the Ionosphere	8
IRRI-06	YenChieh Lin, Numerical modeling of metallic ion species Fe ⁺ , Mg ⁺ , and Na ⁺ and studies of the layer structures in mid-latitude ionosphere.	8
IRRI-07	Goderdzi G. Didebulidze, Formation and behavior sporadic E under the influence of atmospheric gravity waves	9
IRRI-08	Goderdzi G. Didebulidze, Some properties of the TIDs and TADs by observation the oxygen red 630 nm line nightglow intensities from Abastumani	9
IRRI-09	Pei-yun Chiu, Spatial and Temporal Variation of the FORMOSAT-3/COSMIC S4 scintillation index using Tidal Analysis	10
IRRI-10	Andrew Kiene, Numerical modeling of equatorial spread F using observed neutral wind profiles	10
IRRI-11	James Spann, The Scintillation Prediction Observations Research Task (SPORT): A Pathfinder Mission	10
IRRI-12	Diana Loucks, High-latitude GPS Scintillation from E Region Electron Density Gradients during the December 20, 2015 Geomagnetic Storm	11
IRRI-13	Yu Jiao, Equatorial Amplitude Scintillation Spectrum Analysis and Fading Characteristics on GPS Signals	12
IRRI-14	Brandone Ernest Lance, Meso-scale Flow Bursts in the High-Latitude Ionospheric Convection Pattern	12
IRRI-15	Weijia Zhan, On the spectral features of atypical F-region echoes	12

Data Assimilation or Management

DATA-01	Stefan Codrescu, Developing An Ensemble Kalman Filter for Data Assimilation in CTIPE	13
DATA-02	Michelle Salzano, The Antarctic Geospace Data Portal	13
DATA-03	Chih-Ting Hsu, Ionospheric specification and forecast by ensemble assimilation of FORMOSAT-7/COSMIC-2 slant total electron content to a coupled model of thermosphere, ionosphere, and plasmasphere	13
DATA-04	Ryan M. McGranaghan, Reconstruction of three-dimensional auroral ionospheric conductivities via an assimilative technique	14
DATA-05	Marcin Pilinski, A New Assimilative Tool for Specifying Satellite Drag and Orbital Space Weather Conditions	14

Instruments or Techniques for Ionospheric or Thermospheric Observation

ITIT-01	Geoff Crowley, From DICE to DIME: An Evolution of CubeSat Based E-field Instrumentation	15
----------------	-----------------------------------------------------------------------------------------------	----

ITIT-02	Patrick Dandenaull, Comparison of modeled meridional neutral winds using changes in hmF2 with neutral wind observations and other models	15
ITIT-03	Harrison W Bourne, Improved Gradient Based TEC & Receiver Bias Estimation Using the Code Noise & Multipath Correction	16
ITIT-04	Magdalena Louise Moses, Experiment Design to Assess Ionospheric Perturbations During the 2017 Total Solar Eclipse	16
ITIT-05	Marc A. Higginson-Rollins, Diurnal Variation of LF Transmitter Signals at Many Locations	17
ITIT-06	Enrique Luis Alfonso Rojas Villalba, Stochastic modeling of nonlinear dynamics in Farley-Buneman waves	17
ITIT-07	Anthony J. Mannucci, Scientific inference in geophysics and implications for using numerical simulations in scientific investigations	17
ITIT-08	John Swboda, Improvement of Resolution of Incoherent Scatter Radar Using Electronically Scanned Arrays and Inverse Theory	18
ITIT-09	Salih Mehmed Bostan, Preliminary Results of an HF Software Defined Radar System to study D-Region Modification	18
ITIT-10	Jun Wang, Ionosphere Remote Sensing Using Closely Spaced GNSS Arrays ...	19
ITIT-11	Shantanab Debchoudhury, Effects of Additive Noise on Orbital Retarding Potential Analyzers	19
ITIT-12	Gareth Perry, Broadband radio physics experiments at HF with e-POP RRI	19
ITIT-13	Kenneth Zia, OPAL CubeSatellite Flight, Line of Sight Integration, and Atmospheric Modeling	20
ITIT-14	Bo Han, Performance Evaluation of Radio Occultation Data Processing Software in Southeast Asia	20
ITIT-15	Robert Albarran, Kinetic Model of the Auroral Ion Outflow as Observed by the VISIONS Sounding Rocket	22
ITIT-16	Carl Andersen, Measuring Neutral Winds, Turbulence and Diffusion in the Lower Thermosphere with Multi-Point, Chemical-Release Sounding Rocket Payloads	22
ITIT-17	Kang-Hung Wu, Reconstruction of the FORMOSAT-3/COSMIC electron density using empirical orthogonal function	22
ITIT-18	Yi Duann, Photochemical model for atomic oxygen ion retrieval from ground-based observations of airglow	22
ITIT-19	Ting-Han Lin, Improved Calibration Method for System Phase Bias of Chung-Li VHF Radar	23
ITIT-20	John Elliott, Using a Geophysical Inversion with Tristatic Scanning Doppler Imagers	23
ITIT-21	Brian Harding, Ground-based Thermospheric Wind Measurements: sensitivity to Tropospheric Scattering	24
ITIT-22	Lee Joseph Kordella, A new neutral wind sensor for nano-satellite platforms...	24

ITIT-23	Jesse Kane McTernan, A Space-based System for Investigating the Response of Stimulated Ionosphere	24
ITIT-24	Lindsay Victoria Goodwin, Investigating the ion thermodynamics of the F region ionosphere	24
ITIT-25	Meghan Harrington, Initial Results from the RENU2 Sounding Rocket	25
ITIT-26	Dev Raj Joshi, Investigation of the Gravitational Rayleigh Taylor Instability (GRTI) growth rate factors of equatorial plasma bubble irregularities with oblique HF links	25
ITIT-27	Siddharth Krishnamoorthy, Spacecraft communication through high density plasma in the D-region of the Ionosphere during reentry	26
ITIT-28	Julio Alberto Oscanoa, MLT wind estimations obtained from specular and non-specular meteor trails at Jicamarca	26
ITIT-29	Charles Bussy-Virat, Relationship between the drag parameters uncertainties and the orbital position uncertainties for LEO satellites	27
ITIT-30	Jonathan Parham, ANDESITE: Multipoint Measurements of Small Scale Aurora Phenomena with CubSat Formations	27

Long Term Variations of the Ionosphere-Thermosphere

LTVI-01	Eunsol Kim, Tomographic reconstruction of plasmaspheric electron density using JASON-1 plasmaspheric TEC measurements	27
LTVI-02	Steven Brown, Investigation of Ionosonde-Based Indices for a Better Representation of Solar Cycle Variations in IRI	28

MidLatitude Thermosphere or Ionosphere

MDIT-01	Vicki Hsu, Impact of Drag Effects on the Wind and Temperature Structure of the Upper Thermosphere	28
MDIT-02	Chih-Te Hsu, Daytime Ion and Electron Temperatures in the Topside Ionosphere at Middle Latitudes	29

Magnetosphere-Ionosphere-Thermosphere Coupling

MITC-01	Yangyang Shen, Statistical investigation of anisotropic ion temperature enhancements observed by the CASSIOPE/e-POP satellite	29
MITC-02	Yining Shi, Using AMPERE data to understand and verify dayside neutral wind.....	29
MITC-03	Yun-Ju Chen, Plasma and Convection Reversal Boundary Motions in the High Latitude Ionosphere	30
MITC-04	Nithin Sivadas, On the source of energetic electron precipitation during auroral substorms	30

MITC-05	Austin Sousa, Global and Seasonal Assessments of Magnetosphere / Ionosphere Coupling via Lightning-Induced Electron Precipitation	31
MITC-06	Mariangel Fedrizzi, Initial Storm Validation of the Ionosphere-Plasmasphere-Electrodynamics (IPE) Model	31
MITC-07	Boyi Wang, Response of dayside aurora on closed field lines to solar wind driving	31
MITC-08	Jiashu Wu, Field-aligned currents associated with multiple arc systems	32
MITC-09	Spencer Hatch, IMF control of dayside Alfvénic activity in the magnetosphere-ionosphere transition region: FAST observations.....	32
MITC-10	Lucas David Hurd, Effects of measurement resolution and the E-region neutral wind on estimating Joule heating rates in the high-latitude ionosphere/thermosphere	33
MITC-11	Joseph Jensen, Can Particle Precipitation in the Ionosphere Affect the Magnetic Reconnection Rate?	33
MITC-12	Su-In Kim, THEMIS, Van Allen Probes, and Super DARN observations of magnetospheric and ionospheric responses to the Sudden Commencement on Feb 16, 2013	34
MITC-13	Nicholas Perlongo, Ring Current-Ionosphere Coupling: Self-consistent Aurora Validation	34
MITC-14	Jason Ahrens, Characteristics of Equatorward Edge Auroral Waves	34
MITC-15	Hassan Akbari, High Ion Temperature Events Observed by RISR: a Case Study.....	34
MITC-16	Xinzhao Chu, Antarctic neutral Fe layers at thermospheric altitudes up to ~200 km and their correlations to geomagnetic storms and convection electric fields.....	35
MITC-17	Ying Zou, Localized Field-aligned Currents in the Polar Cap Associated with Airglow Patches	35
MITC-18	Yang Lu, Observations of Poynting flux in the dayside cusp region at different altitudes	36
MITC-19	Juha Vierinen, High temporal resolution observations of auroral electron density using superthermal electron enhancement of Langmuir waves	36

Planetary Studies

PLAN-01	Chuanfei Dong, Multifluid MHD study of the solar wind interaction with Mars' upper atmosphere during the 2015 March 8th ICME event	36
PLAN-02	Lynsey Schroeder, Infrasonic Acoustic Wave Propagation in Terrestrial Planetary Atmospheres	37
PLAN-03	Liang Wang, Multi-fluid moment simulation of Ganymede	37
PLAN-04	Jared Bell, Examining the Magnetosphere-Ionosphere coupling processes in the thermospheres of Earth and Jupiter	38

PLAN-05	Jeremy Rioussel, Electrodynamics of the Martian dynamo region near magnetic cusps and loops	38
----------------	---------------------------------------------------------------------------------------------------	----

Polar Aeronomy

POLA-01	Changsup Lee, Polar thermospheric winds and temperature observed by Fabry-Perot Interferometer at Jang Bogo Station, Antarctica	38
POLA-02	Meghan Burleigh, Anisotropic fluid modeling of the VISIONS sounding rocket campaign	39
POLA-03	Burcu Kosar, Analysis of near real-time citizen science observations to validate model predictions of auroral visibility	40
POLA-04	Riley Troyer, High Altitude Antarctic Winds	40
POLA-05	Maimaitirebike Maimaiti, Dynamics of Ionospheric Plasma Convection Under Extreme Northward IMF Conditions	40
POLA-06	Manbharat Singh Dhadly, Seasonal dependence of high latitude upper atmospheric winds: A climatological study based on ground and space based instruments	41
POLA-07	Jeong-Young Ji, General-moment-equation approach to the Coulomb-Milne problem	41

Solar Terrestrial Interactions in the Upper Atmosphere

SOLA-01	Andrea Hughes, Variability of the F-region ionosphere with solar activity	42
SOLA-02	Eun-Young Ji, Comparison of IRI-2012 with JASON-1 TEC and incoherent scatter radar observations during the 2008-2009 solar minimum period	42
SOLA-03	Susan M. Nossal, Observed increase in the Wisconsin northern hemisphere hydrogen emission data set	42
SOLA-04	Nuri Emrahoglu, Geocoronal Balmer-alpha hydrogen emission observations made with the Turkish Dual Etalon Fabry-Perot Spectrometer (DEFPOS)	43
SOLA-05	Justin Yonker, Improving Simulations of Odd Nitrogen in the Upper Atmosphere.....	43
SOLA-06	Ji-Hee Lee, The relationship between high-speed solar wind streams and NO concentration in the upper mesosphere and thermosphere	43
SOLA-07	Derek Gardner, Geocoronal fine-structure cascade excitation constraints for ground-based observations	44
SOLA-08	Liam Kilcommons, Unifying DMSP Space Weather Observations: Field-Aligned Currents (FACs) and Electron Energy Flux organized with respect to IMF orientation and the Central Plasma Sheet Aurora	44

CEDAR Workshop – IT Session Abstracts
Day 1 – Tuesday, June 21, 2016

Equatorial Thermosphere or Ionosphere

EQIT-01 - Estimating equatorial daytime vertical ExB drift velocities from magnetic field variations - by Kassamba Abdel Aziz Diaby

Status of First Author: Student IN poster competition, Masters

Authors: Obrou K. Olivier

Abstract: Accurate measurement and prediction of the vertical plasma drift is important for the study of many physical processes in the low-latitude ionosphere. Equatorial $E \times B$ drift velocities are significant input parameters that go into many ionospheric models, because they help describe vertical plasma motions near the magnetic equator. A previous work done by Anderson et al. (2004) has demonstrated the ability to derive Peruvian longitude sector, daytime vertical $E \times B$ drifts from ground-based magnetometer data and have derived the ΔH versus $E \times B$ relationships.

The present research extends the same method to the West African longitude sector. We use magnetic field data of Conakry, Guinea ($-0.46^\circ, 60.37^\circ$) and Abidjan, Cote d'Ivoire ($-6^\circ, 65.82^\circ$) from the African Meridian B-field Education and Research (AMBER) network.

On the basis of data availability, 9 magnetically quiet days have been analyzed and showed that the Peruvian ΔH versus $E \times B$ relationships is applicable to the West African longitude sector.

EQIT-02 - Global Distribution and Characteristics of Equatorial Plasma Bubbles - by Jonathon Smith

Status of First Author: Student IN poster competition, Masters

Authors: Jonathon Smith, R. A. Heelis

Abstract: Data recorded during the seven year period from 2008 to 2014, a period that spans more than one half of a magnetic Solar cycle and includes solar minimum and a moderate solar maximum, by the Ion Velocity Meter (IVM) as part of the Coupled Ion Neutral Dynamics Investigation (CINDI) aboard the Communication/Navigation Outage Forecasting System (C/NOFS) satellite is used to study equatorial plasma bubbles (EPBS) from 17:00 to 5:00 in altitudes from 350 to 850 km. Here EPBs are identified by profiles in the plasma density, and each may be described by its width in apex longitude, relative density reduction, and the number of local minima within it providing a simple measure of the structure. Here we describe depletion parameters as a function of location and season with the goal to discover the relationships between these parameters and the generation and evolution of the depletions.

EQIT-03 - Parametric Wave Growth in a Hybrid PIC/Fluid Simulation of the Equatorial E Region - by Matthew Young

Status of First Author: Student IN poster competition, PhD

Authors: M. A. Young, M. M. Oppenheim, Y. S. Dimant

Abstract: The Farley-Buneman (FB) and gradient drift (GD) instabilities routinely develop in the partially ionized plasma of the E-region ionosphere, where ion-neutral collisions dominate ion motion while electron

motion is affected by both electron-neutral collisions and the background magnetic field. When the total electric field rises above a threshold determined by the plasma acoustic speed and the ratio of electron to ion mobility, FB waves develop and become turbulent. Even when the electric field is subthreshold for FB instability, the presence of a large-scale density gradient parallel to the total electric field can cause the GD instability to develop. In the equatorial E region, large-scale density perturbations in the plane perpendicular to the magnetic field should produce the necessary gradients and electric fields to drive both FB and GD turbulence. Numerical simulations have been unable to simultaneously resolve GD and FB structure and ionospheric radars, which observe at a single wavelength, must infer kilometer-scale dynamics at from meter-scale observations. We present results from a parallelized hybrid simulation that uses a particle-in-cell (PIC) method for ions while modeling electrons as an inertialess, quasi-neutral fluid. This approach currently allows us to reach length scales of hundreds of meters (with expectation of kilometers in the near future) with sub-meter resolution. However, it requires solving a large linear system derived from a Poisson-like PDE that depends on plasma density, ion flux, and electron parameters. We solve the resultant linear system at each time step via the Portable Extensible Toolkit for Scientific Computing (PETSc). The results of our simulations show growth of density irregularities due to both electric-field-aligned density gradients and electric fields large enough to trigger Farley-Buneman turbulence. This model has immediate applications to radar observations of the E-region ionosphere, as well as potential applications to the F-region ionosphere and the solar chromosphere.

EQIT-04 - Equatorial-PRIMO (Problems Related to Ionospheric Models and Observations) - by Tzu-Wei Fang

Status of First Author: Non-student, PhD

Authors: Tzu-Wei Fang, David Anderson, Tim Fuller-Rowell, Naomi Maruyama, Mihail Codrescu, Ludger Scherliess, Vince Eccles, John Retterer, Joe Huba, Art Richmond, Astrid Maute, Aaron Ridley

Abstract: We do not fully understand all the relevant physics of the equatorial ionosphere, so that current models do not completely agree with each other and are not able to accurately reproduce observations. To understand the strengths and the limitations of theoretical, time-dependent, low-latitude ionospheric models in representing observed ionospheric structure and variability and to better understand the underlying ionospheric physics and develop improved models, we initiated a multi-year Equatorial-PRIMO workshop at the CEDAR meeting. Two sets of ionosphere-plasmasphere models are participated: non self-consistent models including Ionospheric Forecast Model (IFM), Ionosphere-Plasmasphere Model (IPM), Low Latitude Ionosphere Sector Model (LLIONS), Physically Based Model (PBMOD), Global Ionosphere and Plasmasphere (GIP), SAMI2 is Another Model of the Ionosphere (SAMI2), Ionosphere-Plasmasphere-Electrodynamics model (IPE), SAMI3 is Also a Model of the Ionosphere (SAMI3), and self-consistent models including Thermosphere-Ionosphere-Electrodynamics general circulation model (TIE-GCM), Global Ionosphere-Thermosphere Model (GITM), the Coupled Thermosphere Ionosphere Plasmasphere Electrodynamics (CTIPE). For this particular comparison, all the self-consistent models are run under realistic F10.7 and Kp during Nov 7-12, 2012 and Mar 10-15, 2013. Ionospheric parameters including ExB vertical drift, NmF2, hmF2, TEC, and E-region density and thermospheric parameters including O/N2, zonal, and meridional winds from the models are compared with each other and with observations. Overall, these models reproduce reasonable diurnal variation of the thermosphere and ionospheric F-region density. However, the agreements among models and with the observations are rather poor. We will present these results, discuss the differences, and describe our vision of the way forward for Equatorial-PRIMO.

EQIT-05 - Quantifying the sources of ionospheric Day-to-day variability - by Tzu-Wei Fang

Status of First Author: Non-student, PhD

Authors: Tzu-Wei Fang, Tim Fuller-Rowell, Tomoko Matsuo, Valery Yudin

Abstract: Driving the Global Ionosphere Plasmasphere (GIP) model with the thermospheric parameters from the Whole Atmosphere Model (WAM), simulation results show significant longitudinal and day-to-

day variations in the ionospheric parameters. To further quantify the contribution of lower atmosphere, solar and geomagnetic forcing to the ionospheric variability, two sets of simulations at two different seasons (June-July and September-October) are carried out. First, using the fixed solar and geomagnetic activity levels, the contributions of lower atmosphere tides to the longitudinal and day-to-day variability in the upper atmosphere are estimated. Secondly, apply the realistic day-to-day solar and geomagnetic inputs in the models to capture most of the variability in the ionosphere. In this version of model, the TIROS/NOAA auroral precipitation patterns are included and the daily solar irradiance is derived from the SDO/EVE measurements. The standard deviations of the NmF2 at each local time from both runs are calculated and compared with observation. The day-to-day variation of ionospheric parameters including NmF2, hmF2, TEC, and vertical drifts at particular location will be presented. We will also explore the seasonal dependency of the ionospheric variability.

EQIT-06 - Long-duration depletion in the topside ionospheric total electron content during the recovery phase of the March 2015 strong storm - by Jiahao Zhong

Status of First Author: Student IN poster competition, PhD

Authors: Jiahao Zhong, Jiuhou Lei, Wenbin Wang, Xinan Yue, Alan G. Burns and Xiankang Dou

Abstract: Topside ionospheric total electron content (TEC) observations from multiple low Earth orbit (LEO) satellites have been used to investigate the local time, altitudinal and longitudinal dependence of the topside ionospheric storm effect during the recovery phase of the March 2015 geomagnetic storm. The results of this study show that there was a persistent topside TEC depletion that lasted for more than 3 days after the storm main phase at most longitudes, except in the Pacific Ocean region, where the topside TECs during the storm recovery phase were comparable to the quiet-time ones. The observed depletion in the topside ionospheric TEC was relatively larger at higher altitudes in the evening sector and greater at local times closer to midnight. Moreover, the topside TEC patterns observed by MetOp-A (832 km) were different from those seen by other LEO satellites with lower orbital altitudes during the storm main phase and the beginning of the recovery phase, especially in the evening sector. This suggests that the physical processes that control the storm-time behavior of topside ionospheric response to storms are altitude dependent.

EQIT-07 - Simulations of vertical ion-drag effect on neutral winds and compositions at low and middle latitudes - by Qingyu Zhu

Status of First Author: Student IN poster competition, PhD

Authors: Qingyu Zhu, Yue Deng, Astrid Maute, A. D. Richmond

Abstract: The ionospheric electrodynamics plays an important role in modulating the motion of plasma and further changing the neutral winds and neutral compositions due to the neutral-ion friction. Specifically, the effects of vertical ion-drag force on the vertical winds in the equatorial region may contribute to the generation of the crests of equatorial thermosphere anomaly (ETA). However, such effect has not been well studied by most general circulation models (GCMs) currently due to the hydrostatic assumption carried by most GCMs. The non-hydrostatic global ionosphere and thermosphere model (GITM) solves the vertical momentum equation and thus offers the opportunity to study the relative contribution of ion-drag force to the vertical momentum change of vertical winds and compositions in the low latitudes. In this study, we will conduct the simulations with GITM by coupling it with the newly developed 3D ionospheric electrodynamic model to improve the electrodynamics in the mid- and low-latitudes. Particularly, 1) examine the output of 3D ionospheric electrodynamic model by replacing the conductivities by their counterparts in GITM; 2) study the neutral winds and compositions of GITM after introducing the electrodynamics from 3D ionospheric electrodynamic model. The vertical ion-drag effect on neutral winds and compositions at low and middle latitudes will be investigated qualitatively.

EQIT-08 - What drives the electrodynamics of the low-latitude evening ionosphere? -
by Arthur D. Richmond

Status of First Author: Non-student, PhD

Authors: Arthur D. Richmond, William Evonosky, Tzu-Wei Fang, Astrid Maute

Abstract: Neutral and plasma dynamics are strongly coupled in the F region. In the low-latitude evening ionosphere an eastward neutral wind is accelerated by a strong eastward horizontal pressure gradient force that is incompletely balanced by ion drag and viscosity. Plasma convection is driven mainly by the zonal neutral wind in the lower Equatorial Ionization Anomaly (EIA) region, balanced by ion-neutral collisions in the E and lower F regions. Increased night-time E-region conductivity retards both ion convection and neutral winds in the F region. Unless the E-region night-time conductivity is large, the accelerating eastward ion convection draws plasma up from lower apex heights, producing the equatorial F-region pre-reversal enhancement of vertical ion drift.

EQIT-09 - Periodicity in the occurrence of equatorial plasma bubbles - by Jong-Min Choi

Status of First Author: Student NOT in poster competition, Masters

Authors: Hyosub Kil, Young-Sil Kwak, Yong-Ha Kim

Abstract: The quasi-periodic occurrence of equatorial plasma bubbles is understood to indicate the preconditioning of bubbles in the bottomside F region. However, no quantitative investigation has been conducted to identify how often quasi-periodic bubbles occur and how well they represent preconditioning. In this study, we investigated the wave property of bubble occurrence (or spacing between bubbles) by analyzing measurements of ion density taken by the Planar Langmuir Probe on board the Communication/Navigation Outage Forecasting System (C/NOFS) satellite in 2008–2012. The wave property in the bubble occurrence was investigated using the periodograms derived from 664 segments of series of bubbles. The spacing between bubbles, in the majority of segments, is represented by the combination of several wave components. This result indicates that bubbles generally occur in a random fashion. The manner of bubble occurrence does not show any notable variation with longitude and season. Because a consistent wave property does not exist in the occurrence of bubbles, and because the appearance of bubbles in the topside is affected by many factors in addition to preconditioning, bubble occurrence is not a tool useful for identification of the property of preconditioning.

EQIT-10 - Thermospheric wind and temperature measurements using Fabry-Perot Interferometers (FPI) at equatorial region of Ethiopia. - by Fasil Tesema Kebede

Status of First Author: Student IN poster competition, Masters

Authors: John Meriwether, Rafael Mesquita, Baylie Damtie

Abstract: The Doppler shifts and widths of the OI 630nm nightglow emission line are used to study the neutral wind speed and temperature of the thermosphere respectively. The altitude of emission of this line lies between 200 and 300km with peak emission at around 240km, which is the bottom side of F region of the ionosphere. In the thermosphere-ionosphere coupling the motion of neutral particles is known to drive the dynamo field that generate many interesting phenomena at equatorial and low latitude ionosphere. Investigating the nighttime plasma instability, storm-time dynamics, and nature of travelling ionospheric disturbances and solar cycle variability and their impacts on the thermosphere requires the knowledge of the background neutral wind and temperature. Around midnight there would be a maximum temperature, some times equal to the daytime maximum temperature, called Midnight Temperature Maximum (MTM). This phenomenon is a result of the convergence of tides from the lower atmosphere and the neutral wind just over the geographic equator. There are some associated features due to this maximum temperature, such as the midnight pressure bulge, midnight density maximum (MDM), midnight collapse and brightness

wave. All these phenomena would have a great impact on the thermospheric dynamics. This study will characterize the morphology of the neutral wind speed and temperature of the neutral particles at equatorial region of Ethiopia using the Fabry-Perot interferometer located at Bahir Dar.

EQIT-11 - Stormtime effects in the thermospheric neutral winds and temperatures over Brazil - by Daniel J. Fisher

Status of First Author: Student IN poster competition, Masters

Authors: Daniel J. Fisher, Jonathan J. Makela, Ricardo A. Buriti

Abstract: We present a collection of storm-time results from Fabry-Perot interferometer measurements taken over northeast Brazil. Two FPIs have been operating nearly continuously since September 2009, observing the storm-driven effects on the thermospheric neutrals via the redline emission. Analyzing these dynamics are useful in studying the low-latitude forcing from energy input in the auroral region that propagates through the disturbance dynamo mechanism. We use both individual case studies and an epoch analysis approach to track the neutral wind, temperature, and brightness changes associated with storms of varying intensity and local-time onset. This study aims to validate the disturbance dynamo effects seen in satellite-based observations.

EQIT-12 - Probing the equatorial ionospheric valley region fluctuations with Jicamarca ISR and VIPIR ionosonde - by Pablo Reyes

Status of First Author: Student NOT in poster competition, Masters

Authors: Pablo Reyes, Erhan Kudeki

Abstract: The ionosonde measurements at Jicamarca show fluctuations in virtual height and angle of arrival throughout the day and across the ionosphere. The daytime ISR data in the valley region shows a periodic coming and going of the echoes as well as widening and narrowing of the ISR spectra. The variation in angle of arrival of the ionosonde echoes is evidence of the stratified electron density contours being rippled by waves propagating through the ionosphere. These waves seem to be of the same scale of the sheet-like 150-km echoes fluctuations in the ISR data. We investigate the relation between the responses of both instruments by performing combined ISR and ionosonde electron density inversions. This multi-instrument approach will give us a better characterization of the daytime electron density in the equatorial valley region.

EQIT-13 - Airglow observations of the ionosphere from three imagers in South America - by Dustin A. Hickey

Status of First Author: Student IN poster competition, Masters

Authors: Carlos Martinis, Michael Mendillo, Jeffrey Baumgardner, Joei Wroten, and Marco Milla

Abstract: Boston University currently operates four all-sky imagers (ASIs) in South America. These ASIs are constantly collecting nighttime data on the thermosphere, ionosphere, and mesosphere by using a variety of filters. In this study we focus on three of these: one in Villa de Leyva, Colombia (5.6° N, 73.5° W, 16.3° mag lat), one near the magnetic conjugate point of the Villa Leyva ASI in El Leoncito, Argentina (31.8° S, 69.3° W, -19.6° mag lat), and one at the magnetic equator in Jicamarca, Peru (11.95° S, 76.87° W, 0.1° mag lat). We use a narrowband filter at 6300 Å to study plasma density perturbations and irregularities. The majority of irregularities that we are looking at are plasma depletions associated with equatorial spread-F. At Jicamarca we are able to observe depletions associated with bottomside ESF and at Villa de Leyva and El Leoncito we observe depletions associated with topside ESF plumes. We compare concurrent observations of depletions and their zonal velocities at Villa de Leyva and El Leoncito to better

understand how they evolve and vary from hemisphere to hemisphere. At Jicamarca we investigate grouping of depletions and show evidence for the modulation of ESF by large scale waves with wavelengths from 200-600 km.

EQIT-14 – Contribution of Neutral Wind and Electrojet to the Structural Dynamics of Equatorial Ionization Anomaly - by Sovit Khadka

Status of First Author: Student IN poster competition, Masters

Authors: Sovit Khadka, Cesar Valladares, Rezy Pradipta

Abstract: The existence of equatorial zonal eastward electric field and the equatorial geometry of the geomagnetic field lines drives a vertical plasma fountain at the magnetic equator that ultimately create the equatorial ionization anomaly (EIA) in the low latitude ionosphere. The equatorial eastward electric field also drives the daytime equatorial electrojet (EEJ) current while neutral wind controls the pattern of plasma drift via dynamo process. We study the response of EIA to the variability of the EEJ and neutral winds in the American low latitude regions using ground based observations. The EEJ strengths are determined using magnetometers and the trans-equatorial neutral wind profile during the day is estimated using interferometer located near geomagnetic equator. EIA is calculated using total electron content (TEC) data measured by Global Positioning System (GPS) from the Low-Latitude Ionospheric Sensor Network (LISN). We find that the spatial configuration such as strength, shape, amplitude and latitudinal extension of the EIAs are generally affected by equatorial electrojet. Results also show that meridional neutral winds have a significant effect on generation of the asymmetry on EIA crests as seen through TEC distributions.

Irregularities of Ionosphere or Atmosphere

IRRI-01 - Asymmetries in the phase velocity of the E-region plasma irregularities at high southern latitudes - by Victoriya V. Forsythe

Status of First Author: Student NOT in poster competition, PhD

Authors: Victoriya Forsythe, Roman Makarevich

Abstract: The relationship between the occurrence of small-scale ionospheric irregularities in the polar and auroral E region and the plasma convection in the F region is investigated using Super Dual Auroral Radar Network (SuperDARN) radars at high southern latitudes. The information about the F-region velocity is deduced using the map potential algorithm. It is found that some radars within SuperDARN have a well-defined bump-on-tail in the E region velocity distribution due to the presence of the high-velocity E-region echoes of a particular velocity polarity. Detailed correlation analysis is performed to investigate the dependency of the asymmetry of E-region velocity upon the asymmetry in the convection component velocity occurrence. The asymmetry in the distribution of E-region velocities with different polarities is found to be stronger than the F-region asymmetry. The radar groupings due to the asymmetry can be explained in part by their orientation relative to predominant convection pattern.

IRRI-02 - Influence of auroral streamers on rapid evolution of SAPS flows - by Bea Gallardo-Lacourt

Status of First Author: Student NOT in poster competition, Masters

Authors: T. Nishimura, L. R. Lyons, V. Angelopoulos, E. Donovan, J. M. Ruohoniemi, and N. Nishitani

Abstract: An important manifestation of plasma transport in the ionosphere is Subauroral Polarization Streams or SAPS, which are strong westward flow lying just equatorward of the electron auroral oval and

thus of enhanced ionospheric conductivities of the auroral oval. While SAPS are known to intensify due to substorm injections, recent studies showed that large variability of SAPS flow can occur well after substorm onset and even during non-substorm times. These SAPS enhancements have been suggested to occur in association with auroral streamers that propagate equatorward, a suggestion that would indicate that plasma sheet fast flows propagate into the inner magnetosphere and increase subauroral flows. We present auroral images from the THEMIS ground-based all-sky-imager array and 2-d line-of-sight flow observations from the SuperDARN radars that share fields of view with the imagers to investigate systematically the association between SAPS and auroral streamers. We surveyed events from December 2007 to May 2013 for which high or mid-latitude SuperDARN radars were available to measure the SAPS flows, and identified 104 events. For streamers observed near the equatorward boundary of the auroral oval, we find westward flow enhancements of ~ 700 m/s slightly equatorward of the streamers. Our statistical study shows that 60% of the westward flow enhancements are associated with streamers that reach close to the auroral equatorward boundary. In addition, we have found that the majority of the remaining events are flow increases associated with IMF changes. We have also characterized the SAPS flow channel width and timing relative to streamers reaching radar echo meridians. We have found a correlation between westward SAPS flow enhancement and streamer intensity, and also a strong correlation between SAPS flow duration and streamer duration. The strong influence of auroral streamers on rapid evolution of SAPS flows suggests that transient fast earthward plasma sheet flows can lead to westward SAPS flow enhancements in the subauroral region, and that such enhancements are far more common than only during substorms because of the frequent occurrences of streamers under various geomagnetic conditions.

IRRI-03 - Asymmetry in plasma irregularity growth near large-scale gradient reversals -
by Leslie J. Lamarche

Status of First Author: Student NOT in poster competition, Undergraduate

Authors: Leslie J. Lamarche, Roman A. Makarevich

Abstract: Asymmetries in plasma density irregularity generation between the leading and trailing edges of the large-scale plasma density structures in the high-latitude ionosphere are investigated. A model is developed that evaluates the gradient-drift instability (GDI) growth rate differences across the gradient reversal that is applicable at all propagation directions and for the broad range of altitudes spanning the entire lower ionosphere. In particular, the model describes asymmetries that would be observed by an oblique scanning radar near density structures in the polar cap such as polar patches and sun-aligned arcs. The dependencies on the relative orientations between the directions of the gradient reversal, plasma convection, and wave propagation are examined at different altitudinal regions. At all altitudes, largest asymmetries are expected for observations along the gradient reversals, e.g. when an elongated structure is oriented along the radar boresite. The convection direction that results in the strongest asymmetries exhibits a strong dependence on the altitude, with the optimal convection being parallel to the gradient reversal in the E region, perpendicular to it in the F region, and at some angle between these extremes in the transitional region.

IRRI-04 - First report of the afternoon E-region plasma density irregularities in middle latitude - by Tae-Yong Yang

Status of First Author: Student NOT in poster competition, Masters

Authors: Young-Sil Kwak, Hyosub Kil, D.V. Phanikumar, Young-Sook Lee

Abstract: We report, for the first time, the afternoon (i.e., from noon to sunset time) observations of the northern mid-latitude E-region field-aligned irregularities (FAIs) made by the VHF coherent backscatter radar operated continuously since 29 December 2009 at Daejeon (36.18°N, 127.14°E, 26.7°N dip latitude) in South Korea. We present the statistical characteristics of the mid-latitude afternoon E-region FAIs based on the continuous and long-term radar observations. Echo signal-to-noise (SNR) of the afternoon E-region

FAIs is found to be as high as 35 dB, mostly occurring around 100-135 km altitudes. Most spectral widths of the afternoon echoes are close to zero indicating that the irregularities during the afternoon time are not related to turbulent plasma motions. It is observed that the occurrence of the afternoon E-region FAIs has strong seasonal variations with maximal occurrence in summer and minimal occurrence in winter season. And, to investigate the afternoon E-region FAIs - Sporadic E (Es) relationship, the FAIs have been also compared with Es parameters based on observations made from an ionosonde located at Icheon (37.14°N, 127.54°E, 27.7°N dip latitude), which is 100 km north of Daejeon. It is shown that the virtual height of Es ($h'Es$) falls mostly in the height range of 105-110 km and these heights are 5-10 km greater than the FAI bottom side. No relation is found between FAIs SNR and top frequency (fEs) (or blanketing frequency (fEs)). SNR of FAIs, however, is found to be related well with ($fEs - fbEs$).

IRRI-05 - Adaptive-Mesh Imaging of the Ionosphere - by Brian Breitsch

Status of First Author: Student IN poster competition, Undergraduate

Authors: Brian Breitsch, Dr. Jade Morton

Abstract: The ionosphere is an unavoidable pathway for all space-based radio navigation, communication, and sensing systems. Solar and geomagnetic activities as well as ionosphere internal processes cause space weather phenomena associated with irregular structures in the ionosphere plasma. These structures can have adverse effects on radio signals traversing the ionosphere. The global navigation satellite systems (GNSS) signals with their low signal power level and dependence on accurate range measurements are the most vulnerable to ionosphere structures refraction, scattering, and diffraction. High resolution spatial and temporary mapping of the ionosphere structures will advance our understanding of ionosphere physical processes responsible for their creation and evolution and their relationship to solar and geomagnetic activities. Furthermore, it will enable development of advanced technologies to mitigate their effects on space-based radio systems.

The sensitivity of GNSS signals to ionospheric irregularities has led to their widespread adoption to monitor and study ionosphere activities both as ground-based networks and on low earth-orbiting (LEO) satellites. As we enter a new era of satellite navigation, multiple constellations of GNSS with unprecedented global coverage, more resilient signal design, and diverse frequency coverage are becoming available for ionosphere remote sensing. The objective of this proposed project is to develop a novel adaptive mesh imaging method that takes advantage of all new GNSS signals and receiver infrastructure on the ground and on the next-generation radio occultation platform COSMIC-2. Adaptive mesh imaging has previously been applied in geophysics to image fine structures in the Earth's surface. We expect the high-resolution images generated from the developed method can be used to identify small-scale ionosphere plasma structures. Through comparative simulations along with validation from in-situ instruments, we hope to establish and validate adaptive mesh tomography as an effective technique for imaging ionosphere plasma structures.

IRRI-06 - Numerical modeling of metallic ion species Fe⁺, Mg⁺, and Na⁺ and studies of the layer structures in mid-latitude ionosphere - by YenChieh Lin

Status of First Author: Student IN poster competition, PhD

Authors: YenChieh Lin, YenHsyang Chu

Abstract: The objectives of this study are focusing on establishing a numerical model that are capable of simulating primary ion species and electron in mid/low-latitude ionosphere E-F-region. In addition to background densities, the layer structures in ionosphere including sporadic-E layers(Es), intermediate layers, neutral metal layers, thermospheric metal layers and further related scientific questions therein are studied by the “Mid-latitude ionospheric layers model (MLIL)”. The MLIL model is a time dependent theoretical numerical model which comprehensively considering the chemistry in E-F-region with remarkable characteristic of taking chemical reaction cycle of the metallic species Fe, Mg, and Na into

account. Furthermore, the MLIL model is set up in very fine grid points, the thin plasma layers with thickness of 1 km can be well simulated. In this research, in addition to development of the MLIL model, the scientific questions about the formations and mechanisms of the ionosphere layer structures are also studied by MLIL model. One simulation result shows the intermediate layer and the sporadic-E layer are both appearing simultaneously at different heights and the major species constituting the Sporadic-E layers are metallic ion (Fe^+ , Mg^+ , and Na^+) and the minor species are nonmetallic ions (NO^+ , O_2^+). On the contrary, the major species of intermediate layers are nonmetallic ions (NO^+ , O_2^+) and the minor species are metallic ion (Fe^+ , Mg^+ , and Na^+). In addition to the components of the layers, of particular interest is that both numerical results and observational data have found the NO^+ and O_2^+ densities reduction in sporadic-E layers and with characteristic of high O_2^+/NO^+ ratio. These raise the questions of whether the chemical reaction cycles can adequately explain the fundamental difference of layers with respect to ion composition and densities. The descending speeds of intermediate layers are also estimated by MLIL, the results show the speeds of intermediate layer above 140km is about 12~17km/hr and 2~3km/hr at around 120km which is identical with Arecibo observation. Furthermore, The MLIL is adapted to simulate if the thermospheric metal layers is possible appearing in mid-latitude. If it's possible, than what dose the roles play by electric field, tidal windshear, gravity, and diffusion.

IRRI-07 - Formation and behavior sporadic E under the influence of atmospheric gravity waves - by Goderdzi G. Didebulidze

Status of First Author: Non-student, PhD

Authors: Goderdzi G. Didebulidze, Giorgi Dalakishvili, Giorgi Matiashvili

Abstract: The atmospheric gravity waves (AGWs) significantly influence the behavior of the thermosphere ions/electrons. It is shown, that in the lower thermosphere when the background wind present, the AGWs evolving in this wind affect the heavy metallic ions vertical motions and can lead to their convergence into horizontal thin layers and consequently form ionosphere sporadic E (Es). For certain values of the velocity of horizontal back-ground wind, occurring in this region, the declined propagation of the AGWs in the mid-latitude lower thermosphere can cause formation multilayered sporadic E. The distances between such Es layers i.e. distance between locations of maximal ions/electrons densities occur is about one AGWs vertical wavelength.

The observed phenomena like of sporadic E multilayered structures and Es layers downward motions are demonstrated by using 3-D numerical simulations describing Es formation by AGWs.

The formation of quasi-periodic echoes like structures by AGWs evolving in the horizontal inhomogeneous wind and possibility of its ions/electrons density oscillations by smaller periods (smaller than Bunt-Väisälä period), which also is observed phenomena, is shown.

IRRI-08 - Some properties of the TIDs and TADs by observation the oxygen red 630 nm line nightglow intensities from Abastumani - by Goderdzi G. Didebulidze

Status of First Author: Non-student, PhD

Authors: Goderdzi G. Didebulidze, Giorgi Javakhishvili, Maya Todua, Lekso Toriashvili

Abstract: The behavior of the oxygen red OI 630.0 nm line nightglow intensity under influence of atmospheric gravity waves (AGWs) is considered, taking into account nightly changes of the thermosphere meridional wind by observations from Abastumani (41.75 N; 42.82 E). The vortical type perturbations, which can be in situ excited in the inhomogeneous horizontal background wind, are also considered. On the basis of theoretical model, the 630.0 nm line integral intensity variations are estimated taking into account thermosphere wind field changes and atmospheric waves propagation influence on the nighttime ionosphere F2 layer. A possibility of identification of waves propagation from polar and equatorial regions during various helio-geophysical conditions is noted. The cases of detected large scale traveling ionosphere

disturbances -TIDs (mostly generated in the polar regions) and traveling atmospheric disturbances -TADs (which can be generated both in polar and equatorial regions) are demonstrated.

IRRI-09 - Spatial and Temporal Variation of the FORMOSAT-3/COSMIC S4 scintillation index using Tidal Analysis - by Pei-yun Chiu

Status of First Author: Student IN poster competition, Masters

Authors: Pei-yun Chiu, Loren Chang

Abstract: The tides generated from the lower atmosphere can propagate upwards, causing ionospheric perturbations. By using GPS radio occultation (RO) signals, FORMOSAT-3/COSMIC satellites can provide global morphology of the S4 scintillation index, quantifying the distribution of GPS and satellite communications disruptions. In this study, we analyze the the local time and spatial variation of the COSMIC S4 index, and quantify the major variation modes through tidal analysis from 2007 to 2014. The seasonal variations of the S4 index are presented in this method and the tidal signatures examined, to determine their distribution and overall effect on ionospheric scintillation. The global S4 index longitudinal and local time distribution is reconstructed using the results of our tidal analysis, and compared with the zonal mean background in solar minimum year (2009) and solar maximum year (2012), to determine the significance of zonal irregularities resulting from nonmigrating tidal disturbances.

IRRI-10 - Numerical modeling of equatorial spread F using observed neutral wind profiles - by Andrew Kiene

Status of First Author: Student IN poster competition, PhD

Authors: A. Kiene, M. F. Larsen, D. L. Hysell

Abstract: The neutral wind in the F region ionosphere near sunset is known to be a key driver of the nighttime F region plasma instabilities known as Equatorial Spread-F (ESF). Eastward winds drive vertical Pedersen currents that, in turn, drive the Rayleigh-Taylor mechanisms responsible for the large plumes of plasma depletion often seen in ESF events. Recent sounding rocket chemical tracer studies have shown large westward winds and wind shears in the equatorial F region during the period near sunset. Westward winds and shears of these magnitudes are unexpected based on current wind models, which show eastward neutral flow with very small vertical gradients above 200 km. It is typical for ionospheric models to use wind inputs from the Horizontal Wind Model (HWM14) in order to model the development of ESF; however, the zonal wind profiles observed in these experiments are not consistent with this approximation during the transition hours near sunset. The rapid change in the winds across the evening terminator is particularly striking. In this study, we apply the observed chemical tracer neutral wind profiles to an existing ESF model in order to investigate the effects of such large westward winds and shears during the transitional period near sunset on the subsequent development of ESF plumes.

IRRI-11 - The Scintillation Prediction Observations Research Task (SPORT): A Pathfinder Mission - by James Spann

Status of First Author: Non-student, PhD

Authors: James F. Spann (NASA/MSFC), Charles Swenson (USU), Otavio Durão (INPE), Luis Loures (ITA), Rod Heelis (UTD), Rebecca Bishop (Aerospace), Guan Le (NASA/GSFC), Mangalathayil Abdu (ITA), Linda Krause (NASA/MSFC), Clezio Nardin (INPE), Joaquim Costa (INPE), Polinaya Muralikrishna (INPE)

Abstract: Structure in the charged particle number density in the equatorial ionosphere can have a profound impact on the fidelity of HF, VHF and UHF radio signals that are used for ground-to-ground and

space-to-ground communication and navigation. The degree to which such systems can be compromised depends in large part on the spatial distribution of the structured regions in the ionosphere and the background plasma density in which they are embedded.

In order to address these challenges it is necessary to accurately distinguish the background ionospheric conditions that favor the generation of irregularities from those that do not. Additionally we must relate the evolution of those conditions to the subsequent evolution of the irregular plasma regions themselves. The background ionospheric conditions are conveniently described by latitudinal profiles of the plasma density at nearly constant altitude, which describe the effects of ExB drifts and neutral winds, while the appearance and growth of plasma structure requires committed observations from the ground from at least one fixed longitude.

This poster will present an international collaborative CubeSat mission called SPORT that stands for the Scintillation Prediction Observations Research Task. This mission will advance our understanding of the nature of ionospheric structures around sunset to enable improved predictions of disturbances that affect radio propagation and telecommunication signals. The science goals will be accomplished by a unique combination of satellite observations from a nearly circular middle inclination orbit and the extensive operation of ground based observations from South America near the magnetic equator. This CubeSat mission is a pathfinder and will set the stage for a future more robust multiplatform scintillation IT mission.

IRRI-12 - High-latitude GPS Scintillation from E Region Electron Density Gradients during the December 20, 2015 Geomagnetic Storm - by Diana Loucks

Status of First Author: Student IN poster competition, Masters

Authors: Diana Loucks, Scott Palo, Marcin Pilinski, Geoff Crowley, Irfan Azeem

Abstract: With the continuing reduction in seasonal Arctic sea ice extent, increase in ship traffic above the Arctic Circle is expected, which will increase the overall communication and navigation footprint in the region. Ionospheric behavior in the high latitudes can significantly impact Ultra High Frequency (UHF) signals in the 300MHz to 3 GHz band, resulting in degradation of Global Positioning System (GPS) position solutions and satellite communications interruptions. To address these operational concerns, a need arises to identify and understand the ionospheric structure that leads to disturbed conditions in the Arctic. This paper focuses on a case study with the goal of identifying correlative features between GPS scintillation and electron density gradients as seen by ground receivers in Alaska and the Poker Flat Incoherent Scatter Radar (PFISR). An observing campaign was conducted during the time period of the December 2015 winter solstice providing an opportunity to study ionospheric disturbances surrounding the moderate geomagnetic storm of December 20, 2015. This storm was classified by NASA as a G2 storm with the Disturbance Time Index (DST) bottoming out at -170 nT and the Kp Index reaching a peak value of 7. Data from PFISR was analyzed during this period for daily intervals of approximately 10 minutes each, and is used as the basis for determining the ionospheric structure. Additionally, data available from a Connected Autonomous Space Environment Sensor (CASES) dual-frequency GPS receiver at Poker Flat Research Range (PFRR) in Alaska provides phase and amplitude scintillation information that can be used to infer the communications and navigation degradation. To further interpret these observations, Ionospheric Data Assimilation Four Dimensional (IDA4D) and Assimilative Mapping of Ionospheric Electrodynamics (AMIE) assimilative models, as well as imagery from the Poker Flat All-Sky Camera are utilized. Structures in the high-latitude ionosphere are known to change on the order of seconds or less, can be decameters to kilometers in scale, and elongate across magnetic field lines at auroral latitudes. Nominal operations at PFISR give temporal resolution on the order of minutes, and range resolution on the order of tens of kilometers, while the CASES receivers have a 100Hz observation sampling rate and record a phase scintillation index (σ_ϕ) value every 100 seconds. In an effort to bring the PFISR and CASES cadences closer in line with the required temporal resolution, only PFISR's field aligned beam was used to monitor the line of site between a GPS satellite and the ground receiver near magnetic midnight, a time known to correlate with scintillation occurrence, yielding a 15 s spacing between power profiles. A σ_ϕ value was then calculated every second by post-processing the raw CASES phase measurements during the requested

PFISR operational times. Of the nine sets of data taken during the 14-22 December window, the strongest scintillation was recorded on the 21st of December, during the geomagnetic storm recovery phase. PFISR power profiles recorded a strong electron density peak near 137 km altitude and the value associated with this peak changed as much as 80% over a five minute interval. One minute after these changes began, σ_ϕ values also increased, reaching a maximum value of 1.56 cycles at 3.75 minutes before tapering off. Presented here is a discussion of this occurrence including context provided by the PFRR All-Sky Camera, PFRR meridian imaging spectrograph, and IDA and AMIE modeling data. The resulting data analysis shows scintillation features associated with E region electron density gradients.

IRRI-13 - Equatorial Amplitude Scintillation Spectrum Analysis and Fading Characteristics on GPS Signals - by Yu Jiao

Status of First Author: Student IN poster competition, PhD

Authors: Yu Jiao, Dongyang Xu, Charles Rino, Yu (Jade) Morton

Abstract: Most previous GNSS scintillation study has followed two general approaches: physics-based modeling of the signal wave propagation through the ionospheric irregularities; and data-driven statistical analysis of the climatology and morphology of scintillation from ground-based and satellite-based measurements. With the development of GNSS networks around the world, a large amount of scintillation data becomes available, which lead to a large number of studies on climatology and morphology of scintillation. However, there is a disconnection between climatology and theoretical physical model. This poster attempts to address this issue by comparing the theoretical phase screen model with real scintillation data in both frequency and time domains. The results will be beneficial for model validation and scintillation characterization.

IRRI-14 - Meso-scale Flow Bursts in the High-Latitude Ionospheric Convection Pattern - by Brandone Ernest Lance

Status of First Author: Student IN poster competition, Masters

Authors: Brandone Ernest Lance, Roderick Heelis

Abstract: Meso-scale convection features are embedded in the larger scale two-cell convection pattern and may contain flow speeds in excess of the background that represent a significant source of heat and momentum to the neutral atmosphere. In order to approach a description of these features it is necessary to describe the spatial scale size of the flow feature, the speed of the flow and the residence time. Here we present a preliminary investigation of the spatial scale of flow bursts at high latitudes observed by the Defense Meteorological Satellite F13 which describes a dawn-dusk orbit across the northern hemisphere. We examine the distribution of scale sizes in flow features in the auroral zones and polar caps and their relationships to flow cells embedded in the larger scale convection pattern.

IRRI-15 - On the spectral features of atypical F-region echoes - by Weijia Zhan

Status of First Author: Student IN poster competition PhD

Authors: Weijia Zhan, Fabiano Rodrigues
Eurico de Rodrigues de Paula

Abstract: This poster is focused on the spectrum features of radar echoes of equatorial spread F (ESF) during June Solstice and post mid-night conditions, when ESF irregularities are less frequent than their pre-midnight, equinox counterparts. For this investigation, we used measurements made by a 30 MHz coherent backscatter radar interferometer installed in the equatorial site of Sao Luis (2.59° S, 44.21° W, -3.99° dip lat). We selected cases of June solstice and pre-midnight (atypical) ESF events and determined the

characteristics of mean Doppler velocity and spectral width of the echoes associated with those events. We compared the spectral features of the atypical irregularities with those of typical ESF, occurring during equinox and pre-midnight conditions. The results of our analysis will be presented and discussed.

Data Assimilation or Management

DATA-01 - Developing An Ensemble Kalman Filter for Data Assimilation in CTIPE - by Stefan Codrescu

Status of First Author: Student IN poster competition, Undergraduate

Authors: Stefan Codrescu, Mihail Codrescu, Mariangel Fedrizzi

Abstract: We are developing an Ensemble Kalman Filter to assimilate data into the Coupled Thermosphere Ionosphere Plasmasphere and Electrodynamics (CTIPE) model. The Ensemble Kalman Filter (EnKF) approach is useful for approximating the non stationary covariance of the state, especially in high dimensional state spaces like that of CTIPE. Challenges include creating a representative distribution of the state uncertainty in the ensemble, limiting the computational complexity of the scheme, and managing the effects of measurement biases. We present preliminary results in assimilating simulated measurements.

DATA-02 - The Antarctic Geospace Data Portal - by Michelle Salzano

Status of First Author: Student IN poster competition, Undergraduate

Authors: Michelle Salzano, Andrew Gerrard, Gil Jeffer, Allan Weatherwax

Abstract: The Antarctic geospace data portal was created in order to host and distribute data and quicklook plots from the instrumentation located at South Pole Station, McMurdo Station, and the Automated Geophysical Observatories. At this time, all fluxgate magnetometer data from all of the stations are posted for a time period covering the late 1990's to today's synoptic data. In the coming months, additional datasets (e.g., searchcoil magnetometers, photometers, and riometers) will be likewise posted. This data portal, linked through antarcticgeospace.org or directly via antarcticgeospace.njit.edu, is now open to community use.

DATA-03 - Ionospheric specification and forecast by ensemble assimilation of FORMOSAT-7/COSMIC-2 slant total electron content to a coupled model of thermosphere, ionosphere, and plasmasphere - by Chih-Ting Hsu

Status of First Author: Student IN poster competition, PhD

Authors: Chih-Ting Hsu, Tomoko Matsuo, Wenbin Wang, Xinan Yue, Jann-Yenq Liu,

Abstract: The Formosa Satellite 7/Constellation Observing System for Meteorology, Ionosphere and Climate 2 (FORMOSAT-7/COSMIC-2) radio occultation mission can provide high temporal- and spatial-resolution slant total electron content (sTEC) data globally, with six satellites at low inclination orbits and another six at high inclination orbits, planned to be launched on 2016 and 2018, respectively. The FORMOSAT-7/COSMIC-2 sTEC data have a great potential to improve ionospheric data assimilation, thus contributing to numerical space weather prediction. The objective of this study is to assess the value of assimilating FORMOSAT-7/COSMIC-2 radio occultation sTEC data to the practical predictability of the ionosphere through assimilative initialization of a coupled thermosphere-ionosphere-plasmasphere model, the Global-Ionosphere-Plasmasphere/Thermosphere-Ionosphere-Electrodynamics General Circulation Model (GIP/TIEGCM).

For this purpose, Observing System Simulation Experiments (OSSEs) of FORMOSAT-7/COSMIC-2 radio occultation sTEC data are carried out by using Ensemble Kalman Filter (EnKF) to examine how FORMOSAT-7/COSMIC-2 sTEC data inform dynamical and chemical processes of the ionosphere-plasmasphere-thermosphere that lead a reduction in GIP-TIEGCM's error growth.

DATA-04 - Reconstruction of three-dimensional auroral ionospheric conductivities via an assimilative technique - by Ryan M. McGranaghan

Status of First Author: Student IN poster competition, PhD

Authors: Delores J. Knipp, Tomoko Matsuo, Ellen Cousins, Stanley C. Solomon

Abstract: Energy redistribution in the magnetosphere-ionosphere-thermosphere (MIT) system is largely controlled by a complex system of field-aligned, Hall, and Pedersen currents, and the electrodynamic underlying their distributions. Application of Ohm's law to the auroral zone requires knowledge of the ionospheric conductivity, whose estimation has often been simplified by invoking Maxwellian behavior of the impacting particles and height independent conductance. Though these assumptions have allowed us to study height-integrated conductivities (conductances), they have also limited our ability to understand how the MIT system operates as a whole. We are now in a position to address conductivity variations, and thus energy redistribution, in three dimensions (3-D).

We present the first objective analysis of the fully 3-D Hall and Pedersen conductivities for the November 30, 2011 coronal mass ejection event. Our reconstruction relies on a data assimilation scheme that optimally combines Defense Meteorological Satellite Program (DMSP) satellite observations with an error covariance model created from an empirical orthogonal functions (EOFs) analysis of the conductivities. This is the same process used to study two-dimensional (2-D) conductance EOFs in McGranaghan et al. [2015] and assimilative conductance reconstruction in McGranaghan et al. [2016]. A comparison of the 2-D and 3-D results reveal distinct differences and underscores the importance of studying the ionosphere in 3-D.

References:

McGranaghan, R., D. J. Knipp, T. Matsuo, H. Godinez, R. J. Redmon, S. C. Solomon, and S. K. Morley (2015), Modes of high-latitude auroral conductance variability derived from DMSP energetic electron precipitation observations: Empirical orthogonal function analysis *J. Geophys. Res. Space Physics*, 120, 11,013–11,031, doi:10.1002/2015JA021828. McGranaghan, R., D. J. Knipp, T. Matsuo, and E. Cousins (2016), Optimal interpolation analysis of high-latitude ionospheric Hall and Pedersen conductivities: Application to assimilative ionospheric electrodynamic reconstruction, *J. Geophys. Res. Space Physics*, 121, doi:10.1002/2016JA022486.

DATA-05 - A New Assimilative Tool for Specifying Satellite Drag and Orbital Space Weather Conditions - by Marcin Pilinski

Status of First Author: Non-student, PhD

Authors: Geoff Crowley, Mihail Codrescu, Eric Sutton

Abstract: Drastic changes in the neutral density of the thermosphere, caused by geomagnetic storms or other phenomena, result in perturbations of satellite motions through drag on the satellite surfaces. This can lead to difficulties in locating important satellites, temporarily losing track of satellites, and errors when predicting collisions in space (conjunction analysis). As the population of satellites in Earth orbit grows, higher space-weather prediction accuracy is required for critical missions, such as accurate catalog maintenance, collision avoidance for manned and unmanned space flight, reentry prediction, satellite lifetime prediction, defining on-board fuel requirements, and satellite attitude dynamics.

We describe ongoing work to build a comprehensive nowcast and forecast system for neutral density, winds, temperature, and composition. This modeling tool, called Dragster, is based on both first-principles and empirical models of the thermosphere running in real-time and using assimilative techniques to produce a thermospheric nowcast. This software will also produce 72 hour predictions of the global thermosphere-ionosphere system using the nowcast as the initial condition and using near real-time and predicted space weather data and indices as the inputs.

In this poster, we will summarize the Dragster design and assimilative architecture, discuss the assimilation dataset, and present preliminary validation results. Results will be presented in the context of neutral densities along the orbits of several validation satellites. Validation satellites were not used as part of the assimilation-dataset and their perigee altitudes span a range from 200 km to 700 km. Results are compared with several leading atmospheric models including the High Accuracy Satellite Drag Model, which is currently used operationally by the Air Force to specify neutral densities.

Instruments or Techniques for Ionosphere or Thermosphere Observations

ITIT-01 - From DICE to DIME: An Evolution of CubeSat Based E-field Instrumentation - by Geoff Crowley

Presented By: Marcin Pilinski

Status of First Author: Non-student, PhD

Authors: Marcin Pilinski, Erik Stromberg, Chad Fish

Abstract: There is a need for inexpensive and robust space-weather monitoring instruments that can fill upcoming gaps in the Nation's ability to monitor critical space weather parameters and meet requirements for specification and forecasting. Foremost among the parameters that must be measured and specified are electric fields, since they drive the ionospheric behavior at both high and low latitudes, and because there are relatively few ground-based measurements. ASTRA has been funded to prepare a risk-reduction mission for an enhanced version of the electric field instrument for CubeSats. This synergistic opportunity has allowed the team to apply lessons learned from a previous mission (DICE) to address the challenges of making a CubeSat that can deploy E-field booms. In this poster, we present the utility of a constellation of electric field measurements, describe the DICE and DIME SensorSats and their current mission status, review the challenges and lessons learned from the DICE mission, show how these challenges are being addressed for DIME, and compare system capabilities with measurement requirements.

ITIT-02 - Comparison of modeled meridional neutral winds using changes in hmF2 with neutral wind observations and other models - by Patrick Dandenault

Status of First Author: Student IN poster competition, PhD

Authors: Patrick Dandenault, Phil Richards

Abstract: A new empirical model of neutral winds in the mid-latitude thermosphere is being developed. Magnetic meridional neutral winds have been derived using the hmF2 layer height from ionosonde observations using a global ionosonde database of mid-latitude ionosonde measurements that spans 30 years. The database consists of nearly 100 mid-latitude ionosonde sites and the derived wind values at each site have a one-hour time resolution. The neutral winds have been named 'equivalent' winds due to the fact that they are obtained from ionospheric F2 layer heights that may be driven by both neutral winds and/or a vertical drift due to electric fields. This work presents a comparison of the derived equivalent neutral winds with other wind models and meridional neutral wind observations. Understanding the behavior of horizontal neutral winds in the thermosphere is critical to ionospheric modeling. The primary mechanism

by which the neutral winds affect ionospheric densities is the inducement of upward and downward ion drifts along Earth's magnetic fields lines. Changes in the altitude of the ions affect the rate at which ions are lost through recombination. Unfortunately, observations of the neutral winds are relatively scarce as compared to other drivers of the ionosphere, so existing models of the thermospheric neutral winds are limited in their resolution and accuracy. Recent sensitivity studies have shown that the uncertainty in the mid-latitude thermospheric winds alone is sufficient to account for 20-30% of the uncertainty in modeled F-region electron densities or Total Electron Content (TEC). This model is being developed for use with first-principles models to significantly improve the understanding of neutral wind forcing of the thermospheric plasma.

ITIT-03 - Improved Gradient Based TEC & Receiver Bias Estimation Using the Code Noise & Multipath Correction - by Harrison W. Bourne

Status of First Author: Student NOT in poster competition, Masters

Authors: Harrison Bourne, Jade Morton , Frank van Graas

Abstract: This poster presents an improved TEC and receiver inter-frequency bias (IFB) estimation algorithm. The original algorithm was presented in 2015 COUNT Workshop where vertical TEC at a local region was modeled in terms of zenith TEC and contributions from the local TEC spatial derivatives. The zenith TEC, local spatial derivatives, and the receiver IFB are unknowns in the range equations. Least squares solutions are obtained by solving these range equations over a 24 hour period assuming that the IFB remains a constant during the period. However this algorithm is vulnerable to the effects of multipath and code noise. The improved algorithm applies a modified version of the Code Noise Multipath (CNMP) algorithm currently used in WAAS reference stations to reduce the pseudorange noise and multipath from range measurements.

ITIT-04 - Experiment Design to Assess Ionospheric Perturbations During the 2017 Total Solar Eclipse - by Magdalena Louise Moses

Status of First Author: Student IN poster competition, Undergraduate

Authors: Gregory Earle , Nathaniel Frissell

Abstract: On August 21, 2017, there will be a total solar eclipse over the United States traveling from Oregon to South Carolina. Solar eclipses offer a way to study the dependence of the ionospheric density and morphology on incident solar radiation. There are significant differences between the conditions during a solar eclipse and the conditions normally experienced at sunset and sunrise, including the east-west motion of the eclipse terminator, the speed of the transition, and the continued visibility of the corona throughout the eclipse interval. Taken together, these factors imply that unique ionospheric responses may be witnessed during eclipses. These include changes in the ionospheric electric fields, changes in the Total Electron Content (TEC) along paths through the eclipsed region, and variations in the density and altitude of the F2 peak. Several studies over the past century investigated these effects; however, some of the results from these studies are contradictory. These contradictions and the studies' limited spatial resolution leave many fundamental questions unanswered. The advent of several mid-latitude GPS and radar networks in the past few decades, such as the Continuously Operating Reference Station (CORS) system and the Super Dual Auroral Radar Network (SuperDARN) radar system, have enabled ionospheric observations with hitherto unprecedented spatial resolution. Also, the establishment of several nationwide amateur radio reporting systems, such as the Reverse Beacon Network (RBN) that monitors radio wave propagation on the high frequency (HF) bands, offers the potential for evaluating changes in ionospheric conditions with unprecedented spatial resolution. We propose to study the effects of the total solar eclipse on the ionosphere using a combination of GPS receivers, the SuperDARN radar system, HF band amateur radio, and plasma modeling. The overall objectives of this study are to characterize the changes in F-region plasma morphology during the eclipse over a larger spatial domain than any previous eclipse experiment.

In addition, the amateur radio component of our study offers a unique opportunity to further engage the amateur radio community nationwide in a scientific study.

ITIT-05 - Diurnal Variation of LF Transmitter Signals at Many Locations -
by Marc A. Higginson-Rollins

Status of First Author: Student IN poster competition, PhD

Authors: Morris B. Cohen

Abstract: The United States Coast Guard (USCG) operates a national network of radio transmitters that serve as an enhancement to the Global Positioning System (GPS). This network is termed Differential Global Positioning System (DGPS) and uses fixed reference stations as a method of determining the error in received GPS satellite signals and transmits the correction value using low frequency radio signals between 285 kHz and 385 kHz.

In this presentation, we evaluate whether these transmitters can be used as a diagnostic tool for characterizing the D region of the ionosphere, a region of the ionosphere that is inaccessible to continuous in situ measurement techniques. We utilize data from an array of three LF AWESOME receivers located in the southeastern United States. We present the data and find diurnal trends in the amplitude and phase of these transmitters, suggesting that LF DGPS signals contain a significant sky wave that has been reflected from the ionosphere.

ITIT-06 - Stochastic modeling of nonlinear dynamics in Farley-Buneman waves -
by Enrique Luis Alfonso Rojas Villalba

Status of First Author: Student IN poster competition, Undergraduate

Authors: Matthew Young, David Hysell

Abstract: The phase speed saturation of Farley-Buneman waves is studied as an interaction with the random turbulent fluctuations in the background. Instead of solving the nonlinear system, we augment the linearized approximation with a stochastic variable. Using Bourret's averaging technique, we were able to obtain a dynamical system for the expected values of the solution. The phase velocity obtained from this new system is close to the experimental value. This approach seems promising for the study of the influence of plasma turbulence generated by different kinds of instabilities on the mean state of the ionosphere.

ITIT-07 - Scientific inference in geophysics and implications for using numerical simulations in scientific investigations - by Anthony J. Mannucci

Status of First Author: Non-student, PhD

Authors: B. T. Tsurutani, O. P. Verkhoglyadova, X. Meng

Abstract: Scientific knowledge is acquired in geophysics generally without the benefit of controlled experiments. In this poster, we discuss how this affects scientific inference in observation-based investigations, and in studies that use numerical simulations. We develop a specific approach to scientific inference where approximate simultaneity of proposed cause and effect phenomena is used to infer causality. We find that, in general, establishing a causal relationship between two phenomena based on simultaneity requires knowledge of how often simultaneity of these phenomena occurs in the absence of causality. We then extend the discussion to using numerical simulations in the scientific inference process. Numerical simulations of physical processes, because they can simulate the values of observations, are often used to infer what physical processes are occurring in nature. We discuss agreement between model output and observations as a basis for inferring the physical processes underlying the observations. We find

that an important factor to consider, which we here call the “confusion factor,” is how often it may occur that insufficient model representations of the physical processes nevertheless lead to agreement between model computations and observations. We provide rationale for developing models of intermediate or low complexity when using geophysical simulations to reach scientific conclusions.

ITIT-08 - Improvement of Resolution of Incoherent Scatter Radar Using Electronically Scanned Arrays and Inverse Theory - by John Swboda

Status of First Author: Student IN poster competition, Masters

Authors: John Swoboda, Joshua Semeter

Abstract: Incoherent Scatter Radar (ISR) is a sensor modality used in the study of the Ionosphere. This modality sets itself apart in its ability to give direct measurement of the plasma parameters. The newest generation of these sensors, such as the AMISR systems, have been leveraging electronically steerable array (ESA) technology. These arrays allow for pulse-to-pulse steering of the antenna beam to collect data, unlike dish based antennas, which are limited by the need to mechanically scan the antenna. This new paradigm not only allows for more flexibility in the measurement of ionospheric plasma parameters but changes some of the aspects of the space-time sampling of these systems.

Multiple ESA based ISR systems operate currently in the high latitude region where the ionosphere is highly variable across numerous temporal and spatial scales. Because of the highly dynamic nature of the ionosphere in this region, it is important to differentiate between measurement induced artifacts and the true behavior of the plasma. Often three dimensional ISR data produced by ESA techniques are fitted in a spherical coordinate space and then the parameters are interpolated to a Cartesian grid, introducing potential error and impacting the reconstructions of the plasma parameters.

Previously the idea of a full space-time ambiguity function was introduced. This frame work poses the estimate of the of the time domain lags of the intrinsic plasma autocorrelation function as a linear inverse problem with the space-time ambiguity function as a blurring kernel over space and time.

We will discuss use of phased array technology as it relates to ISR and the possibilities of using inverse theory to improve the sensor resolution. Along with this discussion we will present a simulation study where we will reconstruct a two dimensional field of plasma parameters using models of both ESA and dish based systems. A two dimensional field will be reconstructed using simple interpolation techniques already used along with methods that attempt to solve a linear inverse problem in the lags. We will examine the strengths and weakness of each method and determine if we can improve the resolution of these reconstructions.

ITIT-09 - Preliminary Results of an HF Software Defined Radar System to study D-Region Modification - by Salih Mehmed Bostan

Status of First Author: Student NOT in poster competition, PhD

Authors: Julio V. Urbina, John D. Mathews

Abstract: The ionosphere is divided into three different regions and each region is identified by the concentration of ions. The densest region is known as F-region that lies above 150 km altitude. E-region is defined in between 90 km to 150 km and this region is almost 100 times denser than the D-region, which is the lowest region both in terms of density and altitude. E-region and D-region becomes silent at night due to the recombination process and absence of solar radiation. In this poster, details and preliminary results of a software defined radar system to study D-region modification are shown. The radar system is operating at 5.125 MHz and currently uses a modified USRP1 board to collect data.

ITIT-10 - Ionosphere Remote Sensing Using Closely Spaced GNSS Arrays - by Jun Wang

Status of First Author: Student IN poster competition, PhD

Authors: Jun Wang, Yu (Jade) Morton

Abstract: Our previous work has demonstrated that GPS L1 signal carrier phase fluctuations observed from a spaced receiver array can be used to estimate ionosphere irregularity horizontal drift velocities. The gist of the approach is to use a joint frequency analysis technique to generate high-resolution time varying spectrum information for the disturbed signal carrier phase. The objective of this paper is to expand upon the previous efforts by applying the same approach to other GNSS signals. Such an expansion allows the study of the self-consistency of the method and the observation of similarities / differences of GNSS signal diffraction patterns between irregularities structures at different physical scales. The focus of this study is on analyzing the irregularity drift velocity estimations from GPS L1 and L2C signals. Estimation results from GPS L5 and GLONASS L1/L2 bands are also studied based on one of the receiver array pairs. We also compared the estimated results against SuperDARN HF measurements. Improving upon the common techniques in the literature, a more adequate comparison algorithm is developed by projecting each GNSS satellite's ionospheric penetration point (IPP) onto the SuperDARN's field-of-view, and then identify the specific SuperDARN grid to perform the comparison.

ITIT-11 - Effects of Additive Noise on Orbital Retarding Potential Analyzers - by Shantanab Debchoudhury

Status of First Author: Student NOT in poster competition, PhD

Authors: Shantanab Debchoudhury, Dr. Gregory Earle

Abstract: Retarding Potential Analyzers (RPA) will be flown on several upcoming CubeSat missions in the low altitude ionosphere. So studying the performance of RPAs under these conditions are of paramount importance. The RPA generates a current to voltage relationship that is a function of the composition and temperature of constituent ions as well spacecraft potential and velocity profiles. The process of data analysis from these current-voltage (IV) curves require sophisticated fitting routines that can deal with a number of variables. The situation is complicated by the presence of additive noise which results in imperfect instrument measurements. The correct estimation of the actual values of ionospheric parameters is thus heavily dependent of the degree of noise in the instrument. In this study we perform a noise characterization of an RPA with a standard grid geometry. Using a simulated orbit from STK and a standard ionospheric model in IRI, a set of IV curves are generated and subjected to various levels of additive noise. Modeled atmospheric conditions encompass seasonal changes as well as extreme cases likely to be encountered for a flight mission in the lower ionosphere. A standard Levenberg-Marquardt fitting routine is used to estimate temperature, composition, spacecraft potential and velocity parameters and the errors are characterized as a function of signal-to-noise ratio. The essence of the study is to develop an improved understanding of the mean errors expected from the instrument at different noise levels.

ITIT-12 - Broadband radio physics experiments at HF with e-POP RRI - by Gareth Perry

Status of First Author: Non-student, PhD

Authors: G. W. Perry, H. G. James, A. Howarth, G. C. Hussey, J.-P. St.-Maurice, and A. W. Yau

Abstract: The Radio Receiver Instrument (RRI), an integral component of the Enhanced Polar Outflow Probe (e-POP) aboard the Canadian, CAScade, Smallsat and Ionospheric Polar Explorer (CASSIOPE)

satellite, is designed to detect and investigate naturally and artificially generated radio waves over a tuning-range of 10 Hz to 18 MHz. RRI samples over a 30 kHz bandwidth at a rate of 62.5 kHz. It can be tuned and held to a fixed frequency, or it can be swept through a band of frequencies at a maximum tuning rate of 500 Hz. We present results from recent e-POP conjunctions with Super Dual Auroral Radar Network (SuperDARN) radar at Rankin Inlet. During these experiments, the radar cycled through transmitting frequencies of 9.20, 10.21, 11.20, and 12.20 MHz, at a rate of 1 Hz, while RRI swept tuned to the same frequencies at a rate of 4 Hz. The pulses received by RRI show clear signs of dispersion. Amplitude variations are seen on a pulse-by-pulse basis, a time scale of milliseconds, and the O- and X-mode components of the pulses are clearly identifiable. Also, the power received by RRI as a function of SuperDARN transmitting frequency is compared to raytrace solutions constrained by an IRI ionosphere, and used to diagnose the HF propagation conditions in the polar-cap region at the time of the experiment.

ITIT-13 - OPAL CubeSatellite Flight, Line of Sight Integration, and Atmospheric Modeling

- by Kenneth Zia

Status of First Author: Student IN poster competition, Masters

Authors: Kenneth Zia, Preston Hooser, Eric Ashby, Ludger Scherliess, Michael Taylor, and the OPAL team

Abstract: Understanding the Earth's lower thermosphere (altitude range 90km-140km) is of growing interest for many areas of research within the space weather community. The NSF OPAL (Optical Profiling of the Atmospheric Limb) mission is designed to measure temperature profiles by observing the day-time O₂ A-band (~760nm) emissions. This will be achieved using integrated line-of-sight measurements of the A-band through a tangential view of the atmosphere down to ~90km. The OPAL instrument will be flown on a 3U CubeSat and is expected to be launched from the International Space Station (ISS) (~400km altitude). We have used a model of OPAL's position and the attitude of its optical system to investigate the instrument's ability to detect space weather signatures in the temperature data. The prime interest is on the effects of solar storms and atmospheric waves. A combination of models of the line-of-sight and atmospheric O₂ A-band emissions are used to simulate the expected output of the OPAL instrument. This data will then be used to test our ability to resolve the input parameters of the lower thermospheric model. Results of this study will be shown.

ITIT-14 - Performance Evaluation of Radio Occultation Data Processing Software in Southeast Asia - by Bo Han

Status of First Author: Student NOT in poster competition, PhD

Authors: Bo Han, Erry Gunawan, Kay-Soon Low, Yu Morton, Tieh-Yong Koh

Abstract: Global Positioning System (GPS) radio occultation (RO) has evolved from a proof-of-concept to operational constellations providing global weather forecasting, climate monitoring, and ionosphere studies. It is based on the principle that GPS signals traversing the Earth's atmosphere experience bending and delay before reaching GPS receivers on Low Earth Orbit (LEO) satellites. The LEO-receiver-measured carrier phase and amplitude of the GPS signals contain propagation effects from the Earth's atmosphere and can be inverted to signal bending angle and atmospheric refractivity profiles [1][2]. The refractivity profiles of the Earth's atmosphere are useful for weather and climate studies. Since the launch of the proof-of-concept mission GPS/MET in 1995, many RO missions have been launched and their measurements have been widely used [3][4]. The COSMIC (Constellation Observing System for Meteorology, Ionosphere, and Climate) mission, launched in the year 2006, is currently the largest RO mission, producing approximately 2000 RO events distributed around the globe daily [5].

RO data processing generally consists of three steps. First, the carrier phase measured by the GPS receiver is converted to an excess phase measurement by eliminating the GPS and LEO satellites' clock offset and their relative range effects [6]. Second, the excess phase is converted to the bending angle profile of the

neutral atmosphere using geometric and/or wave optics method [7]. Finally, the bending angle profile is converted to a refractivity profile of the atmosphere. There are also other intermediate processing operations, such as filtering of the signal, quality control, ionospheric correction, and optimization of bending angles estimations based on climatology information.

To process the collected RO data, various research centers have developed different software. The processing software used by the COSMIC Data Analysis and Archival Center (CDAAC) is continuously evolving and a set of newly reprocessed COSMIC RO data became available in October 2014. Another processing software, the Radio Occultation Processing Package (ROPP) maintained by the Radio Occultation Meteorology Satellite Application Facilities (ROM SAF), provides an open source RO data processing tool that adopted by many RO missions [8]. The open source characteristic makes ROPP an ideal software to process RO mission data for researchers. The accuracy of ROPP has to be verified in the first place. The objective of this study is just to provide an analysis of the accuracy of the ROPP software. To do so, statistical comparisons are carried out between the 2011 Southeast Asia COSMIC RO data processed using the software by CDAAC and by the ROPP. Bending angle and refractivity are used in the comparison. Local profiles generated using European Centre for Medium-Range Weather Forecasts (ECMWF) are used in the refractivity comparison as a reference.

Comparison results show that both the bending angle and refractivity differences between CDAAC and ROPP processed results exhibit relatively larger standard deviation below 10 km. The mean bending angle and refractivity differences between the two processing software are relatively small with the fractional difference of bending angle and refractivity being smaller than 2% and 1% below 40 km, respectively. Comparison with ECMWF profiles shows that the refractivity standard deviations between ROPP results and ECMWF are comparable to those between CDAAC results and ECMWF. The mean refractivity differences between their processing outputs and ECMWF are smaller than 1%. A hypothesis testing based on t-test is carried out to validate the results' statistical significance. Normalized error covariance is then calculated for the refractivity difference between CDAAC processed results and ECMWF profiles, and between ROPP processed results and ECMWF profiles. The normalized error covariance results show that the ROPP performs slightly poorer than CDAAC at altitude above 30 km, and slightly better at other altitude regions. CDAAC and ROPP processing comparison shows that the different background bending angle models used are the major reasons for the performance difference.

- [1] E. R. Kursinski, G. A. Hajj, J. T. Schofield, R. P. Linfield, and K. R. Hardy, "Observing Earth's atmosphere with radio occultation measurements using the Global Positioning System," *J. Geophys. Res. Atmospheres*, vol. 102, no. D19, pp. 23429–23465, Oct. 1997.
- [2] E. R. Kursinski, G. A. Hajj, S. S. Leroy, and B. Herman, "The GPS radio occultation technique," *Terr. Atmospheric Ocean. Sci.*, vol. 11, no. 1, pp. 53–114, 2000.
- [3] R. Ware, C. Rocken, F. Solheim, M. Exner, W. Schreiner, R. Anthes, D. Feng, B. Herman, M. Gorbunov, S. Sokolovskiy, K. Hardy, Y. Kuo, X. Zou, K. Trenberth, T. Meehan, W. Melbourne, and S. Businger, "GPS Sounding of the Atmosphere from Low Earth Orbit: Preliminary Results," *Bull. Am. Meteorol. Soc.*, vol. 77, no. 1, pp. 19–40, Jan. 1996.
- [4] C. Rocken, R. Anthes, M. Exner, D. Hunt, S. Sokolovskiy, R. Ware, M. Gorbunov, W. Schreiner, D. Feng, B. Herman, Y.-H. Kuo, and X. Zou, "Analysis and validation of GPS/MET data in the neutral atmosphere," *J. Geophys. Res. Atmospheres*, vol. 102, no. D25, pp. 29849–29866, Dec. 1997.
- [5] K. Cook and P. Wilczynski, "COSMIC-2: The future of global navigation satellite system - remote observation (GNSS-RO) sensing," in *Geoscience and Remote Sensing Symposium (IGARSS)*, 2010 IEEE International, 2010, pp. 3825–3828.
- [6] Y.-S. Li, C. Hwang, T.-P. Tseng, C.-Y. Huang, and H. Bock, "A Near-Real-Time Automatic Orbit Determination System for COSMIC and Its Follow-On Satellite Mission: Analysis of Orbit and Clock Errors on Radio Occultation," *IEEE Trans. Geosci. Remote Sens.*, vol. 52, no. 6, pp. 3192–3203, Jun. 2014.
- [7] Y. H. Kuo, T. K. Wee, S. V. Sokolovskiy, C. Rocken, W. S. Schreiner, D. C. Hunt, and R. A. Anthes, "Inversion and Error Estimation of GPS Radio Occultation Data," *J. Meteorol. Soc. Jpn.*, vol. 82, pp. 507–531, 2004.
- [8] I. D. Culverwell, H. W. Lewis, D. Offiler, C. Marquardt, and C. P. Burrows, "The Radio Occultation Processing Package ROPP," *Atmos Meas Tech Discuss*, vol. 8, no. 1, pp. 157–190, Jan. 2015.

ITIT-15 - Kinetic Model of the Auroral Ion Outflow as Observed by the VISIONS Sounding Rocket - by Robert Albarran

Status of First Author: Student IN poster competition, Masters

Authors: Robert Albarran, Matthew Zettergren

Abstract: In this investigation, a guiding-center kinetic model is developed and used in a Monte Carlo scheme to derive particle velocity distributions. The model focuses on the auroral ionosphere where the ion outflow occurs and is designed to digest the data obtained by the VISIONS sounding rocket. VISIONS has the objective to identify the drivers and dynamics of the auroral ion outflow below 1000km. This project serves to advance the instrumentation design and data analysis of sounding rocket and satellite missions. This project proves to be a robust, theoretical tool used to derive velocity distributions which may complement those derived by in-situ observations.

ITIT-16 - Measuring Neutral Winds, Turbulence and Diffusion in the Lower Thermosphere with Multi-Point, Chemical-Release Sounding Rocket Payloads - by Carl Andersen

Status of First Author: Student IN poster competition, PhD

Authors: Mark Conde

Abstract: Sounding rocket payloads capable of deploying multi-point chemical releases provide a unique tool for investigating several properties of the lower thermosphere. This type of payload consists of a collection of sub-payloads that are propelled laterally out of the rocket during flight, each containing a canister of liquid tracer which is dispersed by explosive detonation. The result is a luminous "puff" that can be tracked by triangulation using images taken from several ground stations and can yield measurements of the neutral winds and both turbulent and molecular diffusion near the turbopause.

ITIT-17 - Reconstruction of the FORMOSAT-3/COSMIC electron density using empirical orthogonal function - by Kang-Hung Wu

Status of First Author: Non-student, PhD

Authors: Kang-Hung Wu and Yen-Hsyang Chu

Abstract: The Data Interpolating Empirical Orthogonal Functions (DIEOFs) for the reconstruction of missing data has been applied for the sea surface temperature satellite images in the past decades. Fewer literatures investigate the DIEOFS applied for global ionosphere electron density. The objective of this research was to present the precision and accuracy of DIEOFs for ionospheric electron density. The IRI model was selected to simulate the global distribution of the ionospheric NmF2 from July 2007 to February 2014. We compared IRI electron density with missing data reconstructed by the DIEOFs. The results suggest that DIEOFs method is appropriate for the missing data of the ionospheric satellite. For that, this self-consistent method was selected to reconstruct electron density profiles derived from GPS Radio Occultation (RO) performed by the Constellation Observing System for Meteorology, Ionosphere, and Climate (COSMIC). The results show the EOF-based interpolation algorithm may effectively work on the global ionospheric distribution.

ITIT-18 - Photochemical model for atomic oxygen ion retrieval from ground-based observations of airglow - by Yi Duann

Status of First Author: Student IN poster competition, Masters

Authors: Loren C. Chang, Yi Chung Chiou

Abstract: To study the chemistry and composition of the upper atmosphere, we can utilize airglow emissions from the photochemical reactions of the ions in this region. When the atomic oxygen ions, which are distributed in the ionospheric F region, experience an energy level transition, visible light with a wavelength of 630 nm is released. We used the photometer system built by our team to perform ground-based observations of airglow over the sky of Taiwan at The Lulin Observatory (23°28'07"N, 120°52'25"E) during nighttime. We combined the mean values of our observations every 10 minutes with a photo chemistry model based on the formula derived from the theory of R. Link and L. L. Cogger. With this method, we can estimate how the density of oxygen atomic ions varies with time and altitude. This system will be used for long term observations to study the seasonal variation of upper atmosphere composition.

ITIT-19 - Improved Calibration Method for System Phase Bias of Chung-Li VHF Radar -
by Ting-Han Lin

Status of First Author: Student IN poster competition, Masters

Authors: Ting-Han Lin, Yen-Hsyang Chu, Chin-Lung Su

Abstract: In the past decade, the radar interferometry technique has been the primary method we used at Chung-li VHF radar to identify and locate irregularities. In the interferometry method, the real phase difference of echoes was the most important result we sought. However, the phase difference would be changed in transmission through cables and be affected by weather, temperature or humidity changing. Therefore, the received phase difference would not be the true phase difference.

For the sake of finding the true phase difference of signals, the method of expected echoing region has been introduced for estimating initial system phase bias. This method utilizes the field-aligned properties of sporadic E irregularities to calculate the reasonable region we expect to observe irregularities inside. By comparing the expected echoing region and received echoes in phase plane, the initial system phase bias could be easily determined via manual operation.

We have improved the aforementioned method in this study. In the new method, automatic algorithm is being substituted for manual operation, and the initial system phase bias could be automatically obtained without any artificial error. Moreover, in order to make sure that the improved method could be successfully used to obtain the real initial system phase bias, an easily detectable multirotor with GPS tracker were employed to acquire the phase of echoes. By comparing the temporal variation of both echo phases and GPS locations of multirotor, the true initial system phase bias could be calculated. As expected, the calculated system phase biases from multirotor and improved method are highly similar, the experiment result shows that the improved method is indeed reliable.

ITIT-20 - Using a Geophysical Inversion with Tristatic Scanning Doppler Imagers -
by John Elliott

Status of First Author: Student IN poster competition, Undergraduate

Authors: John Elliott, Mark Conde

Abstract: Currently data is collected from an overlapping network of Scanning Doppler Imagers (SDIs) in arctic polar region that each view 115 locations simultaneously with varying degrees of overlap. A physically motivated Tikhonov regularized geophysical inversion technique is attempted and analyzed against existing basis-fitting and geometric triangulation methods of tristatic wind field approximations. Our geophysical inversion seeks to optimize the structure of the wind estimation by preference of physically reasonable curvature and gradients.

ITIT-21 - Ground-based Thermospheric Wind Measurements: Sensitivity to Tropospheric Scattering - by Brian Harding

Status of First Author: Student IN poster competition, Masters

Authors: Brian J. Harding, Jianqi Qin, Jonathan J. Makela

Abstract: Recent measurements of surprising thermospheric wind features, such as apparent downward winds at midlatitudes during geomagnetic storms [Makela et al., 2014] and at equatorial latitudes during dusk [Fisher et al., 2015], have raised questions regarding the reliability of ground-based thermospheric wind measurements. These measurements are made by observing the Doppler shift of optical airglow emissions. In this work, we develop a radiative transfer code to evaluate the effect of scattering by tropospheric aerosols, and we discuss the conditions under which thermospheric wind measurements are likely to be contaminated. We also present an inversion technique to correct for this effect.

ITIT-22 - A new neutral wind sensor for nano-satellite platforms - by Lee Joseph Kordella

Status of First Author: Student IN poster competition, PhD

Authors: Lee Kordella, Gregory D. Earle, Grant Roth, Robert V. Robertson

Abstract: Virginia Tech has developed an in-situ sensor called the Ram Energy Distribution Detector (REDD, pronounced red-dee) to measure the neutral density, changes in the neutral temperature, the light/heavy composition ratio, and the ram velocity of the neutral gas in the frame of reference of an orbital spacecraft. These are critically undersampled parameters for studying ion-neutral coupling effects that are relevant to a host of geophysical effects in Earth's thermosphere/ionosphere system, including scintillation and equatorial spread-F. Neutral density, temperature, and wind measurements are also critical parameters for understanding spacecraft drag in planetary atmospheres, so the REDD sensor could also be used to better understand such effects in the atmospheres of Mars and other planetary bodies. Here we present the results of subsystem validation through laboratory vacuum testing.

ITIT-23 - A Space-based System for Investigating the Response of Stimulated Ionosphere - by Jesse Kane McTernan

Status of First Author: Student IN poster competition, Masters

Authors: Jesse K. McTernan, Julio V. Urbina, and Sven G. Bilén

Abstract: The OSIRIS (Orbital System for Investigating the Response of the Ionosphere to Stimulation and space weather)-3U mission will investigate space weather phenomena by providing in situ and remote sensing measurements of the stimulated (heated) ionosphere. The HF heater at Arecibo Observatory will stimulate the ionosphere to mimic natural ionospheric irregularities at defined locations and times. OSIRIS-3U's primary objective is to characterize the spatial extent and internal structure of the heated region. The OSIRIS-3U mission has been selected by NASA's CubeSat Launch Initiative and expects to launch in mid 2017. We present innovative solutions to the unique challenges of in situ measurements inherent to the CubeSat platform. Size, mass, and power constraints coupled with non-linear interactions among measurement devices, spacecraft, and the ionosphere require dual-purpose materials that maximize the utility of spacecraft surfaces and other resources while enabling accurate data collection.

ITIT-24 - Investigating the ion thermodynamics of the F region ionosphere - by Lindsay Victoria Goodwin

Status of First Author: Student IN poster competition, Masters

Authors: Lindsay Victoria Goodwin, Jean-Pierre St. Maurice, Mike Nicolls

Abstract: Ion heating by friction with neutral particles is known to have a significant impact on the F region ion temperature in the presence of large electric fields, particularly when the ions become supersonic relative to the neutral background population with which they collide. However, what has not been fully characterized is the impact this heating has on ion temperature anisotropy, as well as the influence of these non-Maxwellian velocity distributions on the shape and interpretation of incoherent radar spectra. To study this, reconstructions of incoherent radar spectra made from Monte-Carlo simulations of velocity distributions are being analyzed along-side radar campaigns capable of giving insight into such things as the collision cross-section of different collisions (such as the resonant charge exchange of O⁺ ions with O). For this research, an experiment was devised to scrutinize the plasma along the magnetic meridian so as to extract electric field and ion temperature information at altitudes where frictional heating plays an important role. The results of this work indicate that, as expected, the line-of-sight component of the plasma drift extracted from different altitudes is consistent throughout the ionosphere above 150 km. However, owing to competition with processes such as heat exchange with electrons, neutral atmospheric uncertainties, and heat conduction from above, extracting information about the effect of frictional heating is difficult unless the electric field is very strong. Here, the first electric field and ion temperature results from these special magnetic meridian scanning modes will be shown.

ITIT-25 - Initial Results from the RENU2 Sounding Rocket - by Meghan Harrington

Status of First Author: Student IN poster competition, PhD

Authors: Kristina Lynch, Marc Lessard

Abstract: RENU2 is a multiple investigator sounding rocket campaign that is designed to transit the cusp region and study particle processes during a neutral upwelling event. The RENU2 payload will make dayside observations between 200 and 600 km altitude in the polar cusp and compare with measurements by the EISCAT Svalbard radars. This project aims to investigate the connection between ion outflows and neutral upwelling from the topside ionosphere and how these affect the variability of neutral particle densities. Low-Earth Orbiting satellites are affected by these regions of enhanced neutral densities which decay their orbits due to satellite drag. Dartmouth's part in this is to provide three top-hat style particle detectors designed to measure the ion distribution functions, temperature enhancements and bulk velocity moments. These measurements will assist in getting an initial assessment of the upwelling process. The following provides the initial ion results from the successful RENU2 launch.

ITIT-26 - Investigation of the Gravitational Rayleigh Taylor Instability (GRTI) growth rate factors of equatorial plasma bubble irregularities with oblique HF links - by Dev Raj Joshi

Status of First Author: Student IN poster competition, Masters

Authors: Dev Joshi, Keith Groves

Abstract: We analyze the data from the Metal Oxide Space Cloud (MOSC) experiment in April-May 2013 conducted by the Air Force Research Laboratory with support of the NASA sounding rocket team to understand the factors influencing the growth rate of Gravitational Rayleigh Taylor Instability (GRTI) believed to be the main cause of equatorial plasma irregularities generally known as spread F. Data from oblique HF radio links, ALTAIR incoherent scatter radar and VHF radar are analyzed to examine the parameters influencing the GRTI growth rate such as the plasma drift velocity, the vertical density gradient and the ion-neutral collision frequency correlating to the scintillation activity in the equatorial ionosphere. We apply numerical ray-tracing to optimize the ionospheric profile to match the delay observations so that actual height of the reflection of the radio waves can be surmised to calculate the parameters in the expression for the GRTI. We also seek to understand the various precursor conditions of the pre-reversal vertical drift and the F-layer bottomside density gradient along perpendicular and quasi-parallel (to B)

paths. ALTAIR incoherent scatter radar scans are used to provide ground truth so that the exact state of the ionosphere can be determined for comparison with the oblique HF links. It was found that the linear growth rate calculated in this manner showed a strong correlation with the integrated scintillation activity as defined by the Total Hourly Mean S4 (THMS4) index. The results suggest that oblique HF links may be exploited for short-term forecasts of low-latitude scintillation activity. The scintillations are significant because they affect radio wave propagation and may impact the performance of satellite communications and navigation links.

ITIT-27 - Spacecraft communication through high density plasma in the D-region of the Ionosphere during reentry - by Siddharth Krishnamoorthy

Status of First Author: Student IN poster competition, PhD

Authors: Siddharth Krishnamoorthy, Sigrid Close

Abstract: Spacecraft entering a dense atmosphere from the vacuum of space undergo severe shock and frictional heating, which ionizes the ambient air molecules that surround the spacecraft. This ionization occurs primarily at the boundary of the mesosphere and D-region of the ionosphere (40-80 km altitude). Highly mobile electrons present in plasma that envelops the spacecraft as a result of the ionization are able to effectively shield applied electromagnetic fields below the plasma frequency, which results in a communications blackout between the ground station and the spacecraft for a period of up to 10 minutes. The reduction of the electron number density in this high density plasma layer ($\sim 1e18$ el/cubic m) in localized pockets may provide the key solving the communications blackout problem. We propose to achieve this density reduction through the application of very strong electric fields, which produces a local reduction in the electron density. The electric field is applied from an arrangement of insulated electrodes, strategically placed near the spacecraft antennas. The field is duty-cycled, so as to avoid hazards associated with plasma sheath breakdown near the electrode. We study the response of the plasma layer to the applied voltage using a Particle-In-Cell (PIC) simulation of the interaction of the plasma with the spacecraft surface. Our simulation results show a large reduction (3-6 orders of magnitude) in the plasma density near the electrode, which provides a temporary, low density window for the transmission of electromagnetic waves from the spacecraft to a ground station. We also discuss preliminary results from an experimental campaign conducted in January 2016 at the L2K plasma wind tunnel facility in Cologne, Germany.

ITIT-28 - MLT wind estimations obtained from specular and non-specular meteor trails at Jicamarca - by Julio Alberto Oscanoa

Status of First Author: Student IN poster competition, Undergraduate

Authors: Julio Oscanoa, Danny Scipi3n, and Marco Milla

Abstract: Many non-specular meteor studies have been conducted with the high-power large-aperture (HPLA) radar at the Jicamarca Radio Observatory (JRO). Here, the authors present a comparative study of MLT winds (90 - 110 km) obtained from non-specular meteor trails detected with this radar and specular trails obtained with the Jicamarca All-Sky METeor system that operates at 30 MHz (JASMET 30).

A coordinated campaign was conducted on the nights of April 27-28 using the HPLA system to detect non-specular meteor trails by combining two different antenna setups: "Meteors" and "MST". In the Meteors mode, the antenna points vertically and wind estimations (between 90-110 km) are obtained through interferometric techniques. In the MST mode, the estimations are done applying Doppler Beam Swinging (DBS) technique to non-coplanar meteor trails for heights between 90-110 km. As in previous studies, the non-specular meteor trails were contaminated by the Equatorial ElectroJet (EEJ). Therefore, the hours with less EEJ contamination were selected for the study.

ITIT-29 - Relationship between the drag parameters uncertainties and the orbital position uncertainties for LEO satellites - by Charles Bussy-Virat

Status of First Author: Student NOT in poster competition, PhD

Authors: Charles Bussy-Virat, Aaron Ridley

Abstract: The prediction of the position and the velocity of low Earth orbit (LEO) satellites and orbital debris has become particularly important as their number has considerably increased. Some space missions that include measurements of the Earth require the knowledge of the state (position and velocity) of the spacecraft that takes the measurements. Collision avoidance is also a major issue that can only be solved with a particular accurate orbit determination of the objects in orbit. The Cyclone Global Navigation Satellite System (CYGNSS) that aims to improve the prediction of tropical cyclones by using a constellation of eight satellites is a good example of a mission that requires a high level of accuracy in the orbit propagation of each of the satellites.

After gravity, the main force acting on LEO satellites is atmospheric drag. The drag force acting on the satellite is directly proportional to the thermospheric density, which is complex to model and predict because of the strong coupling of the thermosphere with the lower atmosphere, the ionosphere (itself driven by the magnetosphere), and the Sun. Therefore, uncertainties in the density are not negligible at these altitudes and are an important cause of the uncertainties on the position of a satellite. The drag coefficient and cross section area are drag parameters that are also hard to model and predict. The goal of the study is to relate the uncertainties in these drag parameters (density, drag coefficient, cross section area) with the uncertainties in the positions of LEO satellites. Ensemble of simulations are run to quantify this relationship.

ITIT-30 - ANDESITE: Multipoint Measurements of Small Scale Aurora Phenomena with CubSat Formations - by Jonathan Parham

Status of First Author: Student IN poster competition, PhD

Authors: J. Brent Parham, Joshua Semeter

Abstract: Small scale plasma phenomena---on the order of hundreds of meter---in the aurora are difficult to resolve with conventional satellite based measurements. Boston University will soon launch a satellite---ANDESITE---that allows for a spatial and temporal resolution at this scale by flying a formation of pico-satellites with on-board three-axis magnetometers. With local measurements spaced only a few hundred meters apart, we can differentiate current density distributions in auroral arcs with less constraints on the assumed geometries. These measurements then allow for a better view into the nature of current filaments and vortex structures as seen by high-resolution ground based optical cameras. Here we discuss the concept of operations of the satellite mission and possible data products that will result along with a timeline to launch. ANDESITE only represents one possible sensor arrangement, and we will also propose follow up missions that consist of actively controlled formations for multi point measurements at these scales in the ionosphere.

Long Term Variations of the Ionosphere-Thermosphere

LTVI-01 - Tomographic reconstruction of plasmaspheric electron density using JASON-1 plasmaspheric TEC measurements - by Eunsol Kim

Presented By: Jee Geonhwa

Status of First Author: Non-student, PhD

Authors: Yong Ha Kim, Geonhwa Jee, Ja Soon Shim

Abstract: The measurement of total electron content (TEC) from the GPS ground-based receivers has been used to conduct computerized ionospheric tomography (CIT). We developed an algorithm of tomography using plasmaspheric TECs (pTECs) measured by GPS receiver onboard the JASON-1 satellite in the altitude region of about 1336 km to 20,200 km. A multiplicative algebraic reconstruction technique (MART) is adopted to invert the measured TEC into electron density along the magnetic flux tube. We estimated two-dimensional structure of the plasmaspheric electron density in the altitude range of 1336 – 20,200 km using the pTEC data collected during the period of 2003 - 2006. The climatological electron density distributions on a longitudinal plane indicate that the plasmasphere contracts with decreasing solar activity and the density is higher in December solstice than June solstice, which is similar to the ionospheric annual anomaly. We will present the climatological characteristics of the plasmaspheric electron density from the reconstructed plasmaspheric electron density distributions such as the variations with local time, season, and solar and geomagnetic activities.

LTVI-02 - Investigation of Ionosonde-Based Indices for a Better Representation of Solar Cycle Variations in IRI - by Steven Brown

Status of First Author: Student IN poster competition, Masters

Authors: Steven Brown , Dieter Bilitza

Abstract: In this study new ionospheric indices are presented for the representation of the solar cycle variation of the F2 peak plasma frequency foF2 and the related F2 peak density NmF2. The indices use different groups of ionosonde stations and follow the methodology for the construction of the "global effective sunspot number" (IG) given by Liu et al. (1982). These new indices are derived using monthly median daytime foF2 ionosonde measurements from selected ionosonde stations and distinguish between Northern and Southern hemispheres. We also investigate the differences in these indices when the URSI-88 model is used for foF2 instead of the CCIR model that was used by Liu et al (1982). This is important because the URSI-88 model is the model recommended in IRI. The effectiveness of these new indices is evaluated with a large volume of ionosonde measurements (96 stations) and their performance is compared to that of the IG12 index, currently used in IRI, and to the widely used F10.7 solar index. For the evaluation, a full model representation is used for foF2 including annual and semi-annual oscillatory terms, linear solar terms and cross terms. Our study shows that improvements of several percent can be achieved with these new indices compared to the IG12 index currently used in IRI.

MidLatitude Thermosphere or Ionosphere

MDIT-01 - Impact of Drag Effects on the Wind and Temperature Structure of the Upper Thermosphere - by Vicki Hsu

Status of First Author: Student NOT in poster competition, PhD

Authors: Jeffrey P. Thayer, Wenbin Wang, Alan Burns

Abstract: Drag forces, ion drag and vertical viscosity, are investigated as drivers of global wind and temperature structure in the upper thermosphere, shedding new light on their roles in affecting neutral dynamics and energetics. Exploiting the coupling of an ionosphere-thermosphere (I/T) model, it is discovered that drag forces in the upper thermosphere can lead to distinctly divergent ageostrophic winds, adjustments in mass, modification of pressure gradients, and a redistribution of energy that significantly alters global thermal structure. Through numerical experiments, it is found that for quiet geomagnetic conditions, the interplay between ion drag and viscosity mainly regulates the large-scale thermal structure of the upper thermosphere. We use the day-night temperature gradient as an example to illustrate the importance of accurate drag specifications in physics-based models in order to properly simulate the I/T system.

MDIT-02 - Daytime Ion and Electron Temperatures in the Topside Ionosphere at Middle Latitudes - by Chih-Te Hsu

Status of First Author: Student IN poster competition, PhD

Authors: Chih-Te Hsu, Roderick Heelis

Abstract: In the topside ionosphere during the daytime, the thermal electrons are directly heated by photoelectron fluxes from the local and conjugate hemispheres. The heat is lost primarily through collisions with the ions, with the loss rate being dependent on the ion mass. Likewise the ions are heated by collisions with the electrons and lost primarily through conduction to lower altitudes. In this work we use a model to aid in further interpretation of observations of the temperature distribution in the 0600–1100 LT sector from 30° to 50° magnetic latitude made by the DMSP satellite F15 from 2004 to 2006. In the observations the plasma temperatures, ionospheric composition and densities are dependent on the solar zenith angle and the solar ionizing radiation. The O⁺ temperature is significantly larger in the presence of a H⁺ dominant plasma suggesting a difference in the H⁺ and O⁺ temperatures. The SAMI2 model is used to reproduce the observed behavior and investigate the mass-dependent effects of the individual heating and cooling processes.

Magnetosphere-Ionosphere-Thermosphere Coupling

MITC-01 - Statistical investigation of anisotropic ion temperature enhancements observed by the CASSIOPE/e-POP satellite - by Yangyang Shen

Status of First Author: Student IN poster competition, PhD

Authors: Yangyang Shen, David Knudsen, Johnathan Burchill, Gordon James, David Miles

Abstract: Terrestrial ion outflow and loss to space is the result of acceleration to escape speed of ionospheric ions that normally are strongly bound to earth through gravity. Previous research suggests this acceleration takes place in multiple steps. We investigate low-energy (<10 eV) ion initial energization process in the topside ionosphere in both hemispheres using data from the SEI, MGF, and RRI instruments onboard the CASSIOPE/e-POP satellite. Using the high-frame-rate (100 Hz) two-dimensional ion distribution function data measured by the SEI, we statistically investigate anisotropic ion temperature enhancements, where ion temperatures perpendicular to B rise by more than 0.5 eV relative to the background values, and study their morphology and Kp dependence. Multiple field-aligned current (FAC) sheets are found to be always associated with these events based on magnetic data from the MGF instrument. For some events, signatures of broad-band extremely low frequency (BBELF) plasma waves, whistler hiss and auroral chorus are detected by the RRI instrument. We study the causal relations between the anisotropic ion temperature increases and the magnitudes of the magnitudes of the FACs and the power spectral density (PSD) of plasma waves.

MITC-02 - Using AMPERE data to understand and verify dayside neutral wind - by Yining Shi

Status of First Author: Student IN poster competition, PhD

Authors: Delores Knipp, Qian Wu, Binzheng Zhang, Liam Kilcommons

Abstract: A geomagnetic quiet time period on June 14, 2011 is studied using magnetic potential and field-aligned currents (FACs) patterns developed from Active Magnetosphere and Planetary Electrodynamics Response Experiment (AMPERE) data. On that date, the HIWIND balloon interferometer, sampling at sub-

auroral latitudes, indicated equatorward neutral winds on dayside high latitude region when thermosphere models expected poleward winds during this time period (Wu, 2012). He reported that unrealistically large dayside heating would be needed to turn the winds to agree with the Thermosphere Ionosphere Electrodynamics Global Circulation Model. Moe and Wu (2014) also suggested that an additional heating source was needed to match the observations. Sheng et al. (2015) showed that the Global Ionosphere Thermosphere General Circulation (GITM) model more closely replicated the measurements, but still required unusually large energy inputs at cusp latitudes. Zhang et al. (to be submitted, 2016) show how the wind reversal can be achieved without the need for extraordinary energy inputs. We provide independent verification of that result by assimilating space-based magnetometer data in the new AMIENext procedure (Matsuo et al, 2015). We generate empirical orthogonal functions (EOFs) from the data to describe the primary variability in magnetic potential and field-aligned currents. The EOFs clearly shows the influence of lobe merging/convection related to negative Bx, positive By and positive Bz IMF configuration.

MITC-03 - Plasma and Convection Reversal Boundary Motions in the High Latitude Ionosphere - by Yun-Ju Chen

Status of First Author: Student NOT in poster competition, PhD

Authors: Y.-J. Chen, R. A. Heelis and J. A. Cumnock

Abstract: Systematic observations of the high latitude ionospheric plasma motion reveal that when a two-cell convection pattern can be identified the interplanetary magnetic field (IMF) has a significant influence on the location of the convection reversal boundary (CRB) and the distribution of the plasma flow across the boundary. We present results from a statistical study of data from the DMSP F13 and F15 satellites over the period from 2000 to 2007 and a case study of multi-satellite (F13, F15 and F17) sampling, that describe the motion of the CRB and the plasma motion with respect to it. During periods of stable southward IMF, a total potential drop less than 10 kV, which is attributed to a viscous-like interaction, is distributed over approximately a 4-h magnetic local time (MLT) region centered at dawn and dusk. With a full range of the IMF configurations, a relatively narrow distribution of plasma drifts across the CRB appears only in the 06-07 h and 17-18 h MLT. Under these conditions equatorward and poleward motions of the CRB are preferred when it is located at the highest and lowest latitudes respectively. These observations may imply the rotation of the dayside merging gap away from local noon toward dawn or dusk and substantial boundary motions in the post-noon and pre-noon local time regions associated with the polar cap expansion and contraction. Consecutive sampling of the CRB location and plasma flow may be used to identify times when the boundary and the plasma move together as suggested by the systematic behavior described earlier.

MITC-04 - On the source of energetic electron precipitation during auroral substorms - by Nithin Sivadas

Status of First Author: Student IN poster competition, PhD

Authors: Nithin Sivadas, Michael Hirsch, Joshua L. Semeter

Abstract: Precipitating auroral electrons are believed to originate mainly from parallel electric fields set up at the auroral acceleration region (AAR) extending up to 20,000 km altitude. However, electrons of energy greater than 30 keV are probably generated by acceleration processes beyond the AAR. Observational evidence for the source location of these energetic electrons are hard to come by. In our current work, we present simultaneous magnetically conjugate measurements of energetic electron spectra estimated at the ionosphere using the Poker Flat Incoherent Scatter Radar and measured at the inner plasmashet by the THEMIS spacecraft. The flux of precipitating electrons of energy greater than 30 keV demonstrate a striking spatio-temporal correlation with that of the inner plasmashet electrons. This suggests that the source of the energetic electrons lie at or beyond the inner plasma sheet, and that the acceleration processes within the auroral acceleration zone don't contribute substantially to their energization. Using simultaneous

THEMIS measurements of wave power, we speculate that the electromagnetic ion cyclotron (EMIC) and Chorus waves are likely candidates for electron acceleration within the inner plasmasheet.

MITC-05 - Global and Seasonal Assessments of Magnetosphere / Ionosphere Coupling via Lightning-Induced Electron Precipitation - by Austin Sousa

Status of First Author: Student IN poster competition, PhD

Authors: Austin Sousa, Dr. Robert Marshall, Dr. Sigrid Close

Abstract: Pitch-angle scattering by radio waves in the VLF (~3-30kHz) band is thought to be a major loss mechanism for energetic radiation-belt electrons. Resonant interactions with Whistler-mode VLF waves can alter the reflection altitude of trapped electrons ~100keV - 1MeV; when a particle reflects at a low enough altitude, it can be removed from the magnetosphere through collisions with ionospheric constituents. Terrestrial lightning provides a natural and constantly-occurring source of VLF waves. Here we present a global assessment of lightning-induced electron precipitation (LEP) due to resonant pitch-angle scattering from whistler-mode waves, which represent a coupling process between the magnetosphere and ionosphere.

We combine an end-to-end model of the LEP process with terrestrial lightning activity data from the GLD360 sensor network to construct a realtime geospatial model of LEP-driven energy deposition into the ionosphere. We explore global and seasonal statistics, provide precipitation estimates across a variety of magnetospheric conditions, and compare the total impact to other magnetospheric loss processes.

MITC-06 - Initial Storm Validation of the Ionosphere-Plasmasphere-Electrodynamics (IPE) Model - by Mariangel Fedrizzi

Status of First Author: Non-student, PhD

Authors: M. Fedrizzi, N. Maruyama, T. Fuller-Rowell, P. Richards, T-W. Fang, M. Codrescu

Abstract: The recently developed Ionosphere-Plasmasphere-Electrodynamics (IPE) model provides time dependent, global, three dimensional plasma densities for nine ion species, electron and ion temperatures, parallel and perpendicular velocities of ionosphere and plasmasphere. The geomagnetic storm high latitude drivers rely on the empirical models of the time-dependent Weimer magnetospheric convection and TIROS/NOAA auroral precipitation patterns. The neutral atmosphere composition and winds come from either empirical the MSIS and HWM models, or the Coupled model of the Thermosphere, Ionosphere, Plasmasphere and electrodynamics (CTIPE). In this study, the IPE model is used to simulate the storm-enhanced densities (SEDs) observed during geomagnetic storm events. Various datasets from ground and space are used to validate the model results. Results from these simulations are used to evaluate the relative importance between electric field, neutral wind and neutral composition in reproducing the SEDs. This study aims to provide new insights into the response of the thermosphere and ionosphere to magnetic storms and improve the understanding of magnetosphere-ionosphere coupling.

MITC-07 - Response of dayside aurora on closed field lines to solar wind driving - by Boyi Wang

Status of First Author: Student IN poster competition, PhD

Authors: Boyi Wang; Toshi Nishimura; Desheng Han; Jacob Bortnik; Wen Li; Larry Lyons; Vassilis Angelopoulos; Yusuke Ebihara

Abstract: Diffuse aurora and throat aurora are two major forms of aurora that are observed equatorward of the dayside discrete auroral oval on closed field lines. Dayside diffuse aurora is driven by pitch angle

scattering of energetic electrons in the dayside magnetosphere by whistler mode waves, and often show transient brightenings. Throat aurora is transient discrete auroral brightening in the dayside region with roughly north-south orientation, extending equatorward of the discrete auroral oval. Throat aurora is associated with enhanced precipitation of low-energy electrons with ~ 100 eV. However, the magnetospheric signatures and the upstream drivers of these localized aurora variations are still open questions. With conjunction observations by multiple Time History of Events and Macroscale Interactions during Substorms (THEMIS) satellites (TH-A, TH-B, TH-C, TH-D, TH-E) and South Pole station all-sky imager (ASI), 4 cases of auroral brightenings (2 diffuse aurora and 2 throat aurora) are identified on Jun. 25th, 2008. In 2 diffuse aurora brightening cases, foreshock ions are found to have a roughly one-to-one relation with brightenings of diffuse auroral intensity. Simultaneously, the localized magnetopause compression signatures and magnetosheath particle penetration are observed around those brightening times, indicating localized magnetosphere compression by foreshock effects and magnetosheath particle penetration to dayside outer magnetosphere for driving diffuse auroral brightening. In the 2 cases with throat aurora, pulses of low-energy ions flowing earthward were found in the dayside magnetosphere, and FTE-like signatures were found in the magnetosheath. These connections suggest that throat aurora reflects transient and localized reconnection, magnetosheath particle penetration, and flow burst.

MITC-08 - Field-aligned currents associated with multiple arc systems – by Jiashu Wu

Status of First Author: Student IN poster competition PhD

Authors: J. Wu, D. Knudsen, M. Gillies, E. Donovan, J. Burchill

Abstract: The field-aligned current (FAC) system associated with auroral arcs provides important information regarding the generator responsible for multiple arc systems, and presumably for individual arcs themselves. We have identified two types of FAC configurations in multiple parallel arc systems using ground-based optical data from the Themis all-sky imagers (ASIs), and magnetometers onboard the Swarm satellites during the period from December 2013 to March 2015. The first type represents a collection of multiple up/down current pairs and the other is an arc system within a broad unipolar upward current sheet. We find that (1) events corresponding to the first FAC type are mainly located in the 23-0 MLT sector, and the second type between 20-22 MLT. (2) The average current intensities for upward and downward currents in the first type are similar (~ 0.16 A/m). However, for the second type, the upward average current intensity (~ 0.32 A/m) is greater than the downward current (~ 0.21 A/m). (3) the average current density is larger in the first type for both upward and downward currents, with the latter, however, having a larger average density than the former in both types. (4) upward currents with more arcs embedded have a larger intensity, although the intensity of upward currents and the number of arcs do not show a linear relationship.

MITC-09 - IMF control of dayside Alfvénic activity in the magnetosphere-ionosphere transition region: FAST observations - by Spencer Hatch

Status of First Author: Student NOT in poster competition, Undergraduate

Authors: Spencer M Hatch ¹, Jim LaBelle ¹, Chris C. Chaston ^{2,3}

1. Department of Physics and Astronomy, Dartmouth College, Hanover, NH, USA
2. Space Sciences Laboratory, University of California, Berkeley, CA, USA
3. School of Physics, University of Sydney, Camperdown, NSW, Australia

Abstract: Several studies in the past two decades have shed light on the behavior and role of Alfvén waves, including the seemingly continual presence of Alfvén waves in the cusp region on the dayside. Several questions about them remain, however, including the nature and efficiency of dayside generation mechanisms of Alfvénic Poynting flux. Using a database of inertial Alfvén waves derived from FAST satellite observations, we explore the response of inertial Alfvén waves to the orientation of the interplanetary magnetic field (IMF), in particular the IMF clock angle. Under large IMF B_y , we find

evidence in support of recent simulations [Zhang *et al.*, 2014] showing that the primary locus of Alfvénic activity on the dayside shifts longitudinally away from the known statistical location of the cusp proper. For example, strongly dawnward IMF (IMF $B_y < 0$) produces an enhanced postnoon Alfvénic signature, and strongly duskward IMF (IMF $B_y > 0$) an enhanced prenoon Alfvénic signature. Under large IMF B_y , we also find evidence of longitudinal bifurcation of soft electron precipitation observed in coincidence with these dayside Alfvén waves. The results of this study are a step toward determining the solar wind/magnetospheric mechanisms responsible for dayside generation of Alfvénic activity and Poynting flux.

MITC-10 - Effects of measurement resolution and the E-region neutral wind on estimating Joule heating rates in the high-latitude ionosphere/thermosphere -
by Lucas David Hurd

Status of First Author: Student IN poster competition, PhD

Authors: Hurd, L. D., M. F. Larsen

Abstract: The small-scale variability in high-latitude electric fields has been attributed to the underestimation of the Joule heating rate by modeling and large-scale experimental observations. The neutral wind field has also been demonstrated to be a non-negligible parameter in Joule heating estimates. Previous studies, however, have not determined the scale at which the variability becomes significant to the overall heating, nor has the neutral wind effects been characterized in detail. We have used high-resolution in-situ data from two sounding rocket campaigns to estimate the altitude-resolved Joule heating rate on spatial scales ranging from hundreds of meters to 50 km during moderate substorm conditions. On-board plasma instrumentation provided measurements of the electric field and conductivity, while chemical tracer releases provided the E-region neutral wind vector. The rocket observations show that the Joule heating rate evolves rapidly, by up to half an order of magnitude, on spatial scales of tens of km and temporal scales of a few minutes. Specifically, it is shown that electric field structure on scales greater than 5 km contributes significantly to the heating estimates. The heating rates calculated at resolutions of 5 km or less are consistently more than a factor of 2 greater than the heating rate estimated for 25 to 50 km resolution over the same regions. In addition, the correlation between the conductivity and electric field is determined to be just as important as the fluctuations in the electric field for estimating the effects of fine structure on the heating. The heating response to the neutral wind field is driven by the dynamical behavior of the electrodynamic parameters, at times decreasing or increasing the estimated heating rate by up to 40% and modifying the heating profile.

MITC-11 - Can Particle Precipitation in the Ionosphere Affect the Magnetic Reconnection Rate? – by Joseph Jensen

Status of First Author: Student IN poster competition, PhD

Authors: Joseph B. Jensen, Joachim Raeder

Abstract: Using OpenGGCM two separate days with average (May 4, 2005) and above average (March 17, 2013) precipitation levels were modeled. The precipitation was then varied by a factor of .1 and 10 while leaving all other model inputs the same. The simulations were compared to study how the earth's magnetosphere changed. It was found that by increasing and decreasing the particle precipitation, the dayside magnetopause location changed by up to one earth radius. To further examine movement of the magnetopause, the reconnection rate was calculated using the Hesse *et al.* [2005] method by integrating the parallel electric field along all magnetic field lines to find the maximum reconnection rate. The reconnection rate changed by up to 30% for some precipitation conditions.

MITC-12 - THEMIS, Van Allen Probes, and Super DARN observations of magnetospheric and ionospheric responses to the Sudden Commencement on Feb 16, 2013 -
by Su-In Kim

Presented By: Hyuck-Jin Kwon
Status of First Author: Non-student, Undergraduate

Authors: Khan-Hyuk Kim, Hyuck-Jin Kwon, Geonhwa Jee, Nozomu Nishitani, Tomoaki Hori

Abstract: One of the most specular source of geomagnetic disturbances is an impact of interplanetary shock (IP shock). After IP shocks arrival, geomagnetic field sharply increases because magnetosphere is compressed by strong solar wind dynamic pressure. In this study, we investigated the plasma motion in the ionosphere measured by Super DARN associated with the passage of the IP shock on Feb 16, 2013. We found that two simultaneous observation of Super DARN, which show different motion in the ionosphere measure at Hokkaido in Japan and Pykkvibaer in Iceland, those are located in the nightside and dayside, respectively. THEMIS and Van Allen Probes (VAPs) observed electric field perturbations deduced by IP shock. Electric field perturbations also show local time dependence identical to ionosphere motion. We consider that the longitudinal dependence of ionospheric plasma motions, can be explained by electric field variations in space.

MITC-13 - Ring Current-Ionosphere Coupling: Self-consistent Aurora Validation -
by Nicholas Perlongo

Status of First Author: Student IN poster competition, PhD

Authors: Nick Perlongo, Aaron Ridley, Michael Liemohn, Roxanne Katus

Abstract: The ring current is an integral component of the magnetosphere-ionosphere (M-I) electrodynamic system. Pitch angle diffusion caused by waves in the inner magnetosphere is the primary source term for the diffuse aurora, especially during storm time. A number of empirical models have been developed to define the subsequent scattering rate of ring current electrons. This study investigates the magnetic local time (MLT) and storm dependent electrodynamic impacts of the diffuse aurora using a comparison between hot electron ion drift integrator (HEIDI) with varying electron scattering rates and real geomagnetic storm events. HEIDI was updated to include a self-consistent auroral model and compared with Dst and hemispheric power indices, as well as auroral electron flux and electric field observations. The results are used to investigate the electrodynamic impact of an accurate description of the diffuse aurora on the M-I system.

MITC-14 - Characteristics of Equatorward Edge Auroral Waves - by Jason Ahrns

Status of First Author: Student NOT in poster competition, PhD

Authors: Jason Ahrns, Donald Hampton

Abstract: Through allsky camera data collected at Poker Flat, Alaska, we identify a large scale eveningside auroral phenomenon that presents itself as a periodic north/south modulation in the equatorward edge of the diffuse electron aurora. These modulations have wavelengths of around 100-200km, propagate westward at around 500-800m/s, and tend to appear around 16:00-19:00MLT. We present several examples, analyzing characteristics such as wavelength and ionospheric drift speed. These structures often have a pulsating region just inside the equatorward boundary. We hypothesize these structures may be indicative of a similar wave structure occurring near a boundary in the eveningside magnetospheric flank.

MITC-15 - High Ion Temperature Events Observed by RISR: a Case Study -
by Hassan Akbari

Status of First Author: Non-student, PhD

Authors: Hassan Akbari, Joshua Semeter

Abstract: Incoherent scatter radars (ISRs) measure the frequency spectrum of the scattered signal from random thermal fluctuations in the ionospheric plasma. Once fitted to a theoretical model, the shape of the spectrum provides estimates of a number of plasma parameters. The theoretical models of the frequency spectrum of the scattered signal have been often developed based on a set of assumptions on the state of the plasma. One of the most common assumptions is that the plasma is in thermal equilibrium consisting of electron and ion populations that can be described by Maxwellian distributions. Such assumptions, however, are commonly violated at high latitudes where interactions between the ionosphere and the magnetosphere result in a very dynamic plasma environment. One example of such violations occurs on the edge of auroral arcs when strong electric fields (~ 100 V/m) drive the ions through neutral particles. Collisions between the two species then cause the ion velocity distribution to deviate from Maxwellian. In such cases, the assumption of thermal equilibrium in the standard ISR fitting procedure results in significant errors in derivation of the plasma parameters. The aim of this study is to employ measurements from the Resolute Bay incoherent scatter radar (RISR) to investigate the ISR spectral anomalies caused by non-Maxwellian ion distributions and estimate the level of errors in estimating the plasma parameters that arise due to the wrong imposed assumption.

MITC-16 - Antarctic neutral Fe layers at thermospheric altitudes up to ~ 200 km and their correlations to geomagnetic storms and convection electric fields -
by Xinzhao Chu

Status of First Author: Non-student, PhD

Authors: Xinzhao Chu, Zhonghua Xu, Jian Zhao, Cao Chen, Ian Barry, and Zhibin Yu

Abstract: Several new discoveries from lidar observations at McMurdo, Antarctica will be reported, especially on the studies of neutral Fe layers in the thermosphere up to nearly 200 km. Comparisons to geomagnetic, solar wind, and ionospheric data reveal a close correlation between the thermospheric Fe layers and geomagnetic storms and convection electric fields. We will explore the driving mechanisms for the formation of such correlations.

MITC-17 - Localized Field-aligned Currents in the Polar Cap Associated with Airglow Patches - by Ying Zou

Status of First Author: Non-student, PhD

Authors: Ying Zou; Yukitoshi Nishimura; Johnathan K. Burchill, David J. Knudsen, Larry R. Lyons; Kazuo Shiokawa, Stephan Buchert, Steve Chen, Michael J. Nicolls, J. Michael Ruohoniemi; Kathryn A. McWilliams; Nozomu Nishitani

Abstract: Airglow patches were recently revealed to be collocated with channels of enhanced anti-sunward ionospheric flows propagating across the polar cap from the dayside to nightside auroral ovals. However, how these flows maintain their localized nature without diffusing away remains unsolved. We examine whether patches and collocated flows are associated with localized field-aligned currents (FACs) in the polar cap by using coordinated observations of the Swarm spacecraft, a polar cap all-sky imager, and SuperDARN radars. We commonly (66% of cases) identify substantial magnetic perturbations indicating FAC enhancements around patches, particularly near the patches' leading edge and center, in contrast to what is seen in the otherwise quiet polar cap. These FACs average ~ 75 km in width and have substantial densities ($0.1-0.2 \mu\text{A/m}^2$). They can be approximated as infinite current sheets that are orientated roughly parallel to patches. They usually exhibit a Region-1 sense, i.e. a downward FAC lying eastward of an upward FAC. With the addition of Resolute Bay Incoherent Scatter (RISR-N) radar data, we find that the

FACs close through Pedersen currents in the ionosphere, consistent with the locally enhanced dawn-dusk electric field across the patch. Our results suggest that ionospheric polar-cap flow channels are imposed by structures in the magnetospheric lobe via FACs, and thus manifest mesoscale magnetosphere-ionosphere coupling embedded in large-scale convection.

MITC-18 - Observations of Poynting flux in the dayside cusp region at different altitudes -

by Yang Lu

Status of First Author: Student IN poster competition, PhD

Authors: Yang Lu, Yue Deng, Cheng Sheng Liam Kilcommons, Delores Knipp, Qq Shi, Xiaocheng Gou, Tian Sheng

Abstract: The observations from Defense Meteorological Satellite Program (DMSP) satellites and Cluster satellites show that the cusp region may or may not have substantial Poynting flux and the quantitative results have strong altitude dependence. Our analysis of DMSP F15 satellites (~800km) data reveals that 47% of 279 cusp crossing events observed a significant downward Poynting flux enhancement ($S > 10$ mW/m²). 85% of the crossings have a clear downward Poynting flux ($S > 3$ mW/m²), and only 3% of the crossings did not show a substantial Poynting flux ($S < 1$ mW/m²). In 49 Cluster (4~8 Re) cusp crossings, 41% observed significant downward Poynting flux enhancement. 71% showed a clear downward Poynting flux and 12% cases did not show a substantial downward pointing flux. Interestingly, 26 (52%) out of the total 49 cases had a certain period with a significant upward Poynting flux in the cusp region. The relationships between Poynting flux and AE index, IMF conditions have also been analyzed. Similar investigation will be applied to the Polar and FAST satellite observations.

MITC-19 - High temporal resolution observations of auroral electron density using superthermal electron enhancement of Langmuir waves - by Juha Vierinen

Presented By: Asti Bhatt

Status of First Author: Non-student, PhD

Authors: Juha Vierinen, Asti Bhatt, Joshua Semeter, Michael Hirsch, Anja Stromme, Shun-Rong Zhang, Phillip Erickson

Abstract: We report high temporal resolution auroral electron precipitation observations using the Sondrestrom incoherent scatter radar. The observations make use of the superthermal electron enhancement of Langmuir waves, which is shown to give accurate observations of the electron density during auroral ionization at a sub-second temporal resolution. This is important when matching to the timescales of auroral precipitation related phenomena, such as energy input into the atmosphere and magnetospheric electron acceleration mechanisms. We describe the measurement technique and show an example observation of auroral precipitation. The results show transients in electron density in the order of a few seconds, which are fully resolved by the plasma-line measurements. An electron precipitation model is used to estimate precipitation energy and flux density. The energetic electron flux during the example event has variations even at short time scales. The results show that electron density profiles derived from plasma lines can be a powerful new observational capability.

Planetary Studies

PLAN-01 - Multifluid MHD study of the solar wind interaction with Mars' upper atmosphere during the 2015 March 8th ICME event - by Chuanfei Dong

Status of First Author: Student NOT in poster competition, PhD

Authors: Chuanfei Dong, Yingjuan Ma, Stephen W. Bougher, Gabor Toth, Andrew F. Nagy, Jasper S. Halekas, Yaxue Dong, Shannon M. Curry, Janet G. Luhmann, David Brain, Jack E. P. Connerney, Jared Espley, Paul Mahaffy, Mehdi Benna, James P. McFadden, David L. Mitchell, Gina A. DiBraccio, Robert J. Lillis, Bruce M. Jakosky, and Joseph M. Grebowsky

Abstract: We study the solar wind interaction with the Martian upper atmosphere during the 2015 March 8th interplanetary coronal mass ejection (ICME) by using a global multi-fluid MHD model. Comparison of the simulation results with observations from Mars Atmosphere and Volatile Evolution (MAVEN) spacecraft show good agreement. The total ion escape rate is increased by an order of magnitude, from $2.05 \times 10^{24} \text{ s}^{-1}$ (pre-ICME phase) to $2.25 \times 10^{25} \text{ s}^{-1}$ (ICME sheath phase), during this time period. Two major ion escape channels are illustrated: accelerated pickup ion loss through the dayside plume and ionospheric ion loss through the nightside plasma wake region. Interestingly, the tailward ion loss is significantly increased at the ejecta phase. Both bow shock and magnetic pileup boundary (BS, MPB) locations are decreased from (1.2R_M, 1.57R_M) at the pre-ICME phase to (1.16R_M, 1.47R_M), respectively, during the sheath phase along the dayside Mars-Sun line. Furthermore, both simulation and observational results indicate that there is no significant variation in the Martian ionosphere (at altitudes $\lesssim 200$ km, i.e., the photochemical region) during this event.

PLAN-02 - Infrasonic Acoustic Wave Propagation in Terrestrial Planetary Atmospheres - by Lynsey Schroeder

Status of First Author: Student IN poster competition, Masters

Authors: Lynsey B. Schroeder and Jonathan B. Snively

Abstract: Through the use of a one-dimensional, nonlinear, compressible planetary atmospheric acoustics model, this study performs investigations of propagating infrasonic acoustic waves through the mesospheres and thermospheres of three terrestrial planets - Earth, Mars, and Venus - in order to quantify the propagation, growth, and dissipation of waves on these planets. Due to their greatly differing ambient conditions and atmospheric compositions, which are here provided by the NASA Global Reference Atmosphere Models (GRAM) [Leslie and Justus, 2011; Justus and Johnson, 2001; Justus et al., 2006], there is significant variation in the behavior of atmospheric acoustic waves, which will be assessed in this study. Furthermore, the effects of propagating infrasonic acoustic waves on neutral atmospheric and D-region ionospheric species layers [Snively, 2013; Marshall and Snively, 2014] are investigated. We assess the observability of naturally-occurring acoustic wave phenomena in the upper-atmospheres of these terrestrial planets. We also assess the potential implications of varied solar and thermospheric conditions on measurable atmospheric acoustic disturbances.

PLAN-03 - Multi-fluid moment simulation of Ganymede - by Liang Wang

Status of First Author: Student NOT in poster competition, PhD

Authors: Kai Germaschewski, Ammar Hakim, Chuanfei Dong, Amitava Bhattacharjee

Abstract: Plasmas in space environments, such as solar wind and Earth's magnetosphere, are often constituted of multiple species. Conventional MHD-based, single-fluid systems, have additional complications when multiple fluid species are introduced. We suggest space application of an alternative multi-fluid moment approach, treating each species on equal footing using exact evolution equations for moments of their distribution function, and electromagnetic fields through full Maxwell equations. Non-ideal effects like Hall effect, inertia, and even tensorial pressures, are self-consistently embedded without the need to explicitly solve a complicated Ohm's law. We have benchmarked this approach in classical test problems like the Orszag-Tang vortex and GEM reconnection problems, while also making significant progress in application to, for example, the magnetosphere of Ganymede. Coupling to state-of-art global simulation codes like OpenGGCM is also underway. This preparatory validation work, though treating only

two species currently, shows the simplicity and power of the multi-fluid moment approach in space applications.

PLAN-04 - Examining the Magnetosphere-Ionosphere coupling processes in the thermospheres of Earth and Jupiter - by Jared Bell

Status of First Author: Non-student

Authors: Jared Bell¹, Anna DeJong², Aaron Ridley³, and Steve Bougher³

¹National Institute of Aerospace, Hampton, VA

²Christopher Newport University, Newport News, VA

³University of Michigan, Ann Arbor, MI

Abstract: Unlike Earth, the energy balance determining the thermospheric temperatures in the outer planets is unknown—leading to the “Energy Crisis” in the upper atmospheres of Jupiter, Saturn, Uranus, and Neptune. Solar EUV/UV heating alone cannot reproduce the temperatures measured directly by the Galileo Probe. One theory is that magnetospheric heating in the Jovian high latitudes is so strong that it can drive a global circulation that transports this energy to the equatorial latitude, providing the required heating to remove this energy gap.

In this poster, we compare and contrast the role of high-latitude magnetosphere-ionosphere coupling and heating mechanisms in order to examine the differences between the upper atmospheres of these two worlds. Jupiter’s stronger magnetic field and intense magnetospheric environment represents a significant enhancement over that of Earth’s, allowing us to model two very different atmosphere-magnetosphere systems. To perform this planetary comparison, we use the Global Ionosphere-Thermosphere Model (GITM) for both Earth and Jupiter to simulate the global composition, winds, and temperatures of both planets.

PLAN-05 - Electrodynamics of the Martian dynamo region near magnetic cusps and loops - by Jeremy Riousset

Status of First Author: Non-student, PhD

Authors: Riousset, J. A., C. S. Paty, R. J. Lillis, M. O. Fillingim, S. L. England, P. G. Withers, and J. P. M. Hale

Abstract: Strong and inhomogeneous remanent magnetization on Mars results in a complex pattern of crustal magnetic fields. The geometry and topology of these fields lead to atmospheric electrodynamic structures that are unique among the bodies of the solar system. In the atmospheric dynamo region (~100–250 km altitude), ions depart from the gyropath due to collisions with neutral particles, while electron motion remains governed by electromagnetic drift. This differential motion of the charge carriers generates electric currents, which induce a perturbation field. The electromagnetic changes ultimately alter the behavior of the local ionosphere beyond the dynamo region. Here we use multifluid modeling to investigate the dynamics around an isolated magnetic cusp and around magnetic loops or arcades representative of the magnetic topology near, for example, Terra Sirenum. Our results show consistent, circular patterns in the electric current around regions with high local field strength, with possible consequences on atmospheric escape of charged particles.

Polar Aeronomy

POLA-01 - Polar thermospheric winds and temperature observed by Fabry-Perot Interferometer at Jang Bogo Station, Antarctica - by Changsup Lee

Status of First Author: Non-student, PhD

Authors: Geonhwa Jee, In-Sun Song, Qian Wu, Hyuck-Jin Kwon, Jeong-Han Kim, Yong Ha Kim

Abstract: We analyze night time neutral winds and temperatures from mesosphere and lower thermosphere (MLT, 87 km and 97 km) to mid-thermosphere (250 km) derived from Fabry-Perot Interferometer (FPI), which was installed at Jang Bogo Station (JBS) in Antarctica. Since the location of JBS changes between polar cap and auroral oval region, observed thermospheric winds above 97 km are strongly controlled by ionospheric plasma convection pattern occurring at corresponding area. We examine wind pattern at 97 km coupled to the convecting high-latitude ionosphere is totally different from one at 87 km where semidiurnal tide overwhelms ion drag forcing in neutral dynamics. For climatological study of neutral wind at polar region, FPI winds are compared with Horizontal Wind Model 2014 (HWM14). Model predicts consistent features of wind at 250 km for seasonal variation of both dawn/dusk zonal wind and midnight meridional wind. In contrast, there are large discrepancies between model and observation in winds at MLT region. Temperatures at 250 km follow geomagnetic activity in regards of dramatic changes on a daily basis and clear seasonal trends also exist. Temperature estimation at 97 km is severely affected by aurora above 160 km while temperatures at 87 km change regardless of geomagnetic and auroral activities. During the great storm on 17 March 2015, thermospheric winds abruptly depart from ion convection pattern associated with changes in the orientation of interplanetary magnetic field (IMF). The thermospheric temperatures have immediate reaction to Kp and AE index variations while there are gradual increases in neutral wind during storm period.

POLA-02 - Anisotropic fluid modeling of the VISIONS sounding rocket campaign - by Meghan Burleigh

Status of First Author: Student IN poster competition, PhD

Authors: M. Burleigh, M. Zettergren, D. Rowland, J. Klenzing

Abstract: Significant amounts of ionospheric plasma can be transported to high altitudes (ion upflow) in response to a variety of plasma heating and uplifting processes. Strong DC electric fields frictionally heat the ion population resulting in anisotropic increases in ion temperature that cause large pressure gradients which push the ions outward and upward. Soft electron precipitation heats ambient, F-region ionospheric electrons creating electron pressure gradients which in turn increase the ambipolar electric field, driving ion upflows. Once ions have been lifted to high altitudes, transverse ion acceleration by broadband ELF waves can give the upflowing ions sufficient energy to escape into the magnetosphere (ion outflow).

The VISIONS (VISualizing Ion Outflow via Neutral atom imaging during a Substorm) sounding rocket was launched on the 7th of February 2013 at 821 UT from Poker Flat, AK into the expansion phase of an auroral substorm. During the flight VISIONS flew through several regions of auroral activity and sensed areas of ion outflow as the rocket crossed multiple auroral arcs and moved into the polar cap. During this time there were observations of transversely flowing ions coincident with a region of DC electric fields. Constrained by in situ measurements and partnered with ground based ISR and ASI data, this flight is modeled by the new anisotropic, 2D, ionospheric fluid model, GEMINI-TIA, to generate greater contextual detail of the state of the ionosphere during these upflow and outflow events.

GEMINI-TIA, developed at Embry-Riddle Aeronautical University, is based on a truncated 16-moment description which solves the conservation of mass, momentum, parallel energy, and perpendicular energy for all species relevant to the E, F, and topside ionospheric regions. The model encapsulates ionospheric upflow and outflow processes through the inclusion of DC electric fields, and empirical descriptions of heating by soft electron precipitation and BBELF waves. Using the VISIONS sounding rocket campaign measurements to seed GEMINI-TIA, the types and amounts of upflowing and outflowing ions can be calculated as well as the overall conditions in the ionosphere necessary to reproduce the observations. The VISIONS sounding rocket campaign provides an excellent validation opportunity for this model.

POLA-03 - Analysis of near real-time citizen science observations to validate model predictions of auroral visibility - by Burcu Kosar

Status of First Author: Non-student, PhD

Authors: Burcu Kosar, Elizabeth A. MacDonald, Nathan A. Case, Rodney Viereck, and Yongliang Zhang

Abstract: Since its initial launch in late 2014, the citizen science project Aurorasaurus has been actively collecting ground-based reports of aurora observations from all over the world. A recent study by Case et al., [2016] compared a subset of these citizen science reports with the operational forecast of the visible aurora provided by NOAA's Space Weather Prediction Center (SWPC). The aurora forecast product of SWPC utilizes the output from OVATION (Oval Variation, Assessment, Tracking, Intensity, and Online Nowcasting) Prime (2010) auroral precipitation model for estimating the location of the most equatorial latitude of the visible aurora known as the "view-line". This study demonstrated that 60% of the positive aurora observations collected by Aurorasaurus were equatorward of the "view-line" predicted by SWPC and this finding led to defining a new observation-based Aurorasaurus view-line.

In this presentation, analysis of observations collected by the Aurorasaurus project during the course of one year will be reported and these citizen science reports will then be used to validate model predictions of auroral visibility. This study is an extension to the prior work by covering a much larger data set. Additional data is important for reducing the uncertainties in fits that govern the location of the observational view-line. Furthermore, initial results of a case study comparing citizen science reports with the auroral boundaries obtained from OVATION Prime model and FUV auroral data from SSUSI will be presented for the March 17, 2015 geomagnetic storm.

POLA-04 - High Altitude Antarctic Winds - by Riley Troyer

Status of First Author: Student IN poster competition, Undergraduate

Authors: Riley Troyer, Mark Conde, Don Hampton, William Bristow, Michael Kosch, Theo Davies, Mamoru Ishii

Abstract: In December 2015 and January 2016 the University of Alaska installed two new all-sky imaging Fabry-Perot spectrometers in Antarctica at McMurdo and South Pole stations. The instruments view airglow and auroral emissions from Earth's upper atmosphere. Using high-resolution Doppler spectroscopy they infer wind and temperature fields at the emission altitudes. Emissions from atomic oxygen at 558 nm and 630 nm are used to sense conditions at around 120 km and 240 km altitude respectively. Both sites are located at similar magnetic latitudes (80S vs 74S) but significantly different geographic latitudes (78S vs 90S). Both are typically located near the equator-ward edge of the polar cap during quiet and moderate geomagnetic conditions. Here we will present preliminary observations of F-region (240 km altitude) wind and temperature fields recorded by the two instruments during the first few months of operation, and examine whether any systematic differences appear in the wind or temperature behavior that may be attributed to their differing geographic latitudes.

POLA-05 - Dynamics of Ionospheric Plasma Convection Under Extreme Northward IMF Conditions - by Maimaitirebike Maimaiti

Status of First Author: Student NOT in poster competition, Masters

Authors: Maimaitirebike Maimaiti, J. Michael Ruohoniemi

Abstract: Many previous studies have demonstrated that high-latitude ionospheric convection is strongly influenced by interplanetary magnetic field (IMF) conditions. However, the dynamics of changing convection and the relationship to magnetic reconnection on the magnetopause is relatively unexplored. In this study, we analyze an interval of strong northward IMF on September 9th, 2014 which provided a rare

opportunity to examine variations in the dayside reverse convection throat for an extended period of time. Between 18:00 - 20:00 UT the northward face of the Resolute Bay Incoherent Scatter Radar (RISR-N) was located in the noon sector, and directly measured reverse convection in the dayside throat region. Nearly simultaneous measurements from DMSP satellites confirm the reverse convection and the cusp features expected for northward IMF. Time-series comparison of the north-south flows with the IMF Bz component shows a remarkably high correlation, suggestive of very strong linear coupling, with no sign of velocity saturation. Specifically, as the IMF turned northward and then steadily strengthened to 28 nT, the north-south flows responded linearly, peaking at a maximum value of 2800 m/s. Several small and short lived variations in Bz also produced linear responses in the north-south flows. Likewise, the IMF By component was highly correlated with the east-west ionospheric flows measured by RISR-N. However, time-lagged correlation analysis reveals that the IMF By influence acted on a time-scale which was 10 minutes faster than that of the Bz component. We attribute this difference in time-scales to the occurrence of magnetic merging at two different magnetopause sites as determined by favored merging geometries for the two components of the IMF.

POLA-06 - Seasonal dependence of high latitude upper atmospheric winds: A climatological study based on ground and space based instruments -

by Manbharat Singh Dhadly

Status of First Author: Non-student, PhD

Authors: Manbharat Singh Dhadly, John Emmert, Douglas Drob

Abstract: We seek to understand how quiet-time high latitude upper atmospheric wind circulation responds in magnitude and shape to the changes in seasons. Previous studies have focused on data from individual instruments. In this study, we combine extensive observations of upper thermospheric winds recorded by 12 ground (optical remote sensing) and space based (optical remote sensing and in situ) instruments at northern high latitudes: seven ground based Fabry-Perot interferometers, two Scanning Doppler imagers, and three satellite instruments (UARS/WINDII, DE-2/WATS, and GOCE). These data sets provided enough coverage to accurately model quiet time ($K_p \leq 3$) high latitude horizontal wind patterns as a function of latitude and local time in magnetic coordinates. The preliminary results show that the resulting wind patterns agree well with the observational data used in constructing this climatology, with no major discrepancies among the datasets. The patterns indicate the strong influence of ionospheric convection, with a prominent anticyclonic cell on the dusk side of the magnetic pole and a weaker tendency toward a cyclonic cell on the dawn side. There is also a marked seasonal variation in the patterns. During winter seasons, the neutral wind circulation pattern is confined to only higher latitudes (≥ 70 degree magnetic latitude); it expands to lower latitudes during summer time.

POLA-07 - General-moment-equation approach to the Coulomb-Milne problem -

by Jeong-Young Ji

Status of First Author: Non-student, PhD

Authors: Jeong-Young Ji, Hankyu Lee, Geonhwa Jee

Abstract: Recently, an infinite hierarchy of general moment equations has been developed [1,2]. A great advantage of the general moment method is to provide exact evaluation of the Coulomb (Landau, Fokker-Planck) collision operator. In solving a truncated set of moment equations, a natural convergence scheme is provided by increasing the number of moments. The general moment method is applied to the Coulomb-Milne problem. The moments are expanded in a power series of the altitude and the expansion coefficients are obtained by solving the general moment equations. It is shown that the higher order coefficients require more moments for convergent results. In the interest of generalizing the discontinuous background to a realistic, smoothly varying continuous background, a fluid model of the minor ion species and its closure

scheme are discussed. The fluid model may deal with the effects of particle, energy, and momentum sources.

[1] J.-Y. Ji and E. D. Held, Phys. Plasmas 13, 102103 (2006).

[2] J.-Y. Ji and E. D. Held, Phys. Plasmas 16, 102108 (2009).

Solar Terrestrial Interactions in the Upper Atmosphere

SOLA-01 - Variability of the F-region ionosphere with solar activity - by Andrea Hughes

Status of First Author: Student IN poster competition, PhD

Authors: Andr ea Hughes, Jeffrey Klenzing, Russell Stoneback, and Dieter Bilitza

Abstract: It is well known that the ionosphere varies with a number of inputs, including longitude, latitude, local time, and the solar cycle. In this study we consider the behavior of the ionosphere during the recent solar minimum in 2008, especially in comparison to periods of higher solar activity (e.g., 2011). Also of interest to our study is the ability of empirical models, such as the International Reference Ionosphere (IRI), to capture this variability in the ionosphere. To accomplish our goal we analyzed radio occultation data from the Constellation Observing System for Meteorology, Ionosphere, and Climate (COSMIC) satellite. We considered median electron density values for 81 days surrounding the 2008 and 2011 December solstices. Using the COSMIC dataset, we created global maps of the mid- and low-latitude F-region of the ionosphere, specifically focusing on maximum electron densities (NmF2) and the corresponding altitudes (hmF2). We constructed these maps in Python using the Python Science Analysis Toolkit (pysat). We compare our results with the IRI model and consider ways to improve upon the performance of the model during periods of solar extremes.

SOLA-02 - Comparison of IRI-2012 with JASON-1 TEC and incoherent scatter radar observations during the 2008-2009 solar minimum period - by Eun-Young Ji

Status of First Author: Non-student, PhD

Authors: Eun-Young Ji, Geonhwa Jee, and Changsup Lee

Abstract: The 2008-2009 solar minimum period was unprecedentedly deep and extended. We compare the IRI-2012 with global TEC data from JASON-1 satellite and with electron density profiles observed from incoherent scatter radars (ISRs) at middle and high latitudes for this solar minimum period. For the global mean ionosphere, global daily mean TECs are calculated from JASON-1 TECs to compare with the corresponding IRI TECs during the 2008-2009 period. It is found that IRI underestimates the global daily mean TEC by about 20-50%. The comparison of global TEC maps further reveals that IRI overall underestimates TEC for the whole globe except for the low-latitude region around the equatorial anomaly, regardless of season. The underestimation is particularly strong in the nighttime winter hemisphere where the ionosphere seems to almost disappear in IRI. In the daytime equatorial region, however, the overestimation of IRI is mainly due to the misrepresentation of the equatorial anomaly in IRI. Further comparison with ISR electron density profiles confirms the significant underestimation of IRI at night in the winter hemisphere.

SOLA-03 - Observed increase in the Wisconsin northern hemisphere hydrogen emission data set - by Susan M. Nossal

Status of First Author: Non-student, PhD

Authors: Susan Nossal², Edwin Mierkiewicz³, Fred Roesler¹, R. Carey Woodward², Derek Gardner¹, Matt Haffner¹

¹ University of Wisconsin-Madison

² University of Wisconsin-Fond du Lac

³ Embry-Riddle Aeronautical University

Abstract: Ground-based Fabry-Perot observations of hydrogen airglow emissions taken from northern mid-latitudes indicate solar cycle variation and also suggest an observed underlying increase in the thermospheric hydrogen airglow emission. The approximate 35% increase in hydrogen emission intensity between two solar maxima is larger than would be accounted for by greenhouse gas increases. Other processes may contribute to this increase. The corroboration of the absolute intensity calibration, as well as an improved tropospheric scattering code and method for determining the emission due to cascade excitation indicate the likelihood that none of these experimental factors would account for the apparent increase in the Wisconsin northern hemisphere hydrogen emission data set. We will discuss our efforts to improve the accuracy of the data comparisons, as well as to interpret the observations in the context of modeling of the solar cyclic and climatic influences on upper atmospheric atomic hydrogen and hydrogen containing molecules.

SOLA-04 - Geocoronal Balmer-alpha hydrogen emission observations made with the Turkish Dual Etalon Fabry-Perot Spectrometer (DEFPOS) - by Nuri Emrahoglu

Status of First Author: Non-student, PhD

Authors: Nuri Emrahoglu, Cukurova University, Adana Turkey
Muhittin Sahan, Korkut Ata University, Osmaniye Turkey
Susan Nossal, University of Wisconsin-Madison

Abstract: Geocoronal hydrogen Balmer-alpha emission observations were made with a dual etalon Fabry-Perot spectrometer (DEFPOS) from the TUBITAK National Observatory (TUG) between the years 2003-2004. The TUBITAK National Observatory is located on the Bakiritepe mountain in Antalya, Turkey (36 ° 51'N, 30 ° 20'E, at an altitude of 2547 m). The field of view (FOV) of the DEFPOS instrument is 4.76 degrees. The DEFPOS points in the zenith and observations were taken with 1200 second exposure times. We will describe analysis of the zenith geocoronal hydrogen Balmer-alpha emission observations made using the DEFPOS Fabry-Perot from the TUBITAK National Observatory between 2003-2004.

SOLA-05 - Improving Simulations of Odd Nitrogen in the Upper Atmosphere - by Justin Yonker

Status of First Author: Student NOT in poster competition, PhD

Authors: Scott Bailey

Abstract: Nitric oxide is an important contributor to radiative cooling, ozone loss, and electron density in the upper atmosphere. It is shown that improvements to the chemical rate coefficients, branching ratios, and temperature dependences in TIEGCM can significantly improve agreement with data from the Student Nitric Oxide Explorer (SNOE). The effect of these modifications on the ion and electron density is also evaluated.

SOLA-06 - The relationship between high-speed solar wind streams and NO concentration in the upper mesosphere and thermosphere - by Ji-Hee Lee

Status of First Author: Non-student, Masters

Authors: Ji-Hee Lee, Young-Sil Kwak, Geonhwa Jee, Young-Suk Lee

Abstract: The solar wind is a stream of plasma released from the upper atmosphere of the Sun. The solar wind is divided into two components: slow and fast solar winds. The fast solar wind is thought to originate from coronal holes, which are funnel-like regions of open field lines in the Sun's magnetic field. The physical characteristics of fast solar wind are closely related to variations in space environments including the Earth's magnetosphere and the upper and lower atmospheres. Although its effects are not as strong as solar energetic particle events such as flare and CME, the high-speed solar wind stream more prevalently occurs and may affect the atmospheric chemistry. In this study, we analyzed the NO concentration obtained by MIPAS onboard the ENVISAT according to solar wind speed measured by ACE satellite from 2007 to 2008 winter time in order to study on the atmospheric effects of the high-speed solar wind streams. We report a preliminary result of this analysis.

SOLA-07 - Geocoronal fine-structure cascade excitation constraints for ground-based observations - by Derek Gardner

Status of First Author: Student NOT in poster competition, PhD

Authors: Derek Gardner, Ed Mierkiewicz, Fred Roesler, Susan Nossal

Abstract: Night-time time-averaged Geocoronal Balmer-alpha line-shapes, obtained by Fabry Perot, indicate a decrease in cascade-contribution to the total Balmer-alpha observed intensity with viewing geometry (shadow altitude). Accurately accounting for cascade's redwing line-shape contribution is critical to interpreting individual line-shape observations for residual exospheric dynamic signatures. Poor cascade (or Galactic background) model fits can mask sought after dynamics, leading to misinterpretation of the Balmer-alpha line profile and erroneously high effective exospheric temperatures retrieved from the data-model fits.

Mierkiewicz et al. (2012) empirically demonstrated the percent cascade contribution amounted to 5% (+/- 3%), but a shadow altitude dependence was not clear. Roesler et al. (2014) showed relative cascade contributions to Balmer-alpha profiles could be determined with near simultaneous Balmer-beta observations. Roesler et al (2014) also noted that, due to multiple scattering differences in geocoronal hydrogen for Lyman-beta and Lyman-gamma (responsible for Balmer-alpha and Balmer-beta respectively), there is a trend for the cascade to become a smaller fraction of the Balmer-alpha intensity at larger shadow altitudes.

Here, we show agreement with this shadow altitude dependence using time-averaged Fabry-Perot line profile data. In lieu of actual coincident Balmer-beta observations, we use this reduced data (and Galactic background knowledge from WHAM database) to parameterize the cascade contribution to the Balmer-alpha line profile as a function of shadow altitude. We also quantify retrieved temperature errors when the cascade parameterization is ignored in the model. This cascade parameterization scheme could be useful for instruments that cannot directly resolve the cascade's fine structure components.

SOLA-08 - Unifying DMSP Space Weather Observations: Field-Aligned Currents (FACs) and Electron Energy Flux organized with respect to IMF orientation and the Central Plasma Sheet Aurora - by Liam Kilcommons

Status of First Author: Student NOT in poster competition, Undergraduate

Authors: Liam Kilcommons, Delores Knipp, Robert Redmon

Abstract: We have reprocessed data from the Defense Meteorology Satellite Program magnetometer (SSM) and particle precipitation (SSJ) instruments as part of a NASA effort to bring DMSP space weather observations to the space science community via the CDAWeb virtual observatory. These revised data also include current best measurement uncertainty estimates.

We have used these now publicly available data sets to study location and intensity of the precipitating electron energy flux and the field-aligned currents observed when the spacecraft are within the auroral oval compared to when the spacecraft are equatorward and poleward of the auroral boundary, as a function of solar wind conditions.

The location of the auroral boundary is determined using the DMSP SSJ precipitating electrons and ions instrument, implementing an algorithm which makes use of the newly-derived uncertainty estimates. Magnetic perturbations from the boom-mounted DMSP SSM magnetometer instruments are recomputed using the improved-accuracy spacecraft locations, and used to compute large-scale field-aligned currents using the Minimum Variance Analysis technique. By removing the signatures of the large-scale current systems from the magnetic perturbations we are also able to estimate intensity and scale-size of the smaller-scale currents.

We analyze the field-aligned current density from 3 DMSP spacecraft for several years beginning in 2010, and compare the locations and intensities with those of precipitating electrons as measured by SSJ. The location and intensity variation with solar wind conditions are studied by sorting each spacecraft polar pass by dominant interplanetary magnetic field (IMF) orientation. We examine each IMF category by season, and show a strong seasonal dependence for certain IMF orientations. We also briefly explore the correlation between FAC/precipitation intensity and thermospheric density perturbations.

Ahrns, Jason, 34
Akbari, Hassan, 34
Albarran, Robert, 22
Andersen, Carl, 22

Bell, Jared, 38
Bostan, Salih, 18
Bourne, Harrison, 16
Breitsch, Brian, 8
Brown, Steven, 28
Burleigh, Meghan, 39
Bussy-Virat, Charles, 27

Chen, Yun-Ju, 30
Chiu, Pei-yun, 10
Choi, Jong-Min, 4
Chu, Xinzhao, 35
Codrescu, Stefan, 13
Crowley, Geoff, 15

Dandenault, Patrick, 15
Debchoudhury, Shantanab, 19
Dhadly, Manbharat, 41
Diaby, Kassamba Abdel Aziz, 1
Didebulidze, Goderdzi, 9
Dong, Chuanfei, 36
Duann, Yi, 22

Elliott, John, 23
Emrahoglu, Nuri, 43

Fang, Tzu-Wei, 2
Fedrizzi, Mariangel, 31
Fisher, Daniel, 5
Forsythe, Victoriya, 6

Gallardo-Lacourt, Bea, 6
Gardner, Derek, 44
Goodwin, Lindsay, 24

Han, Bo, 20
Harding, Brian, 24
Harrington, Meghan, 25
Hatch, Spencer, 32
Hickey, Dustin, 5
Higginson-Rollins, Marc, 17
Hsu, Chih-Te, 29
Hsu, Chih-Ting, 13
Hsu, Vicki, 28
Hughes, Andrea, 42
Hurd, Lucas, 33

Jensen, Joseph, 33
Ji, Eun-Young, 42
Ji, Jeong-Young, 41
Jiao, Yu, 12

Joshi, Dev, 25

Kebede, Fasil, 4
Khadka, Sovit, 6
Kiene, Andrew, 10
Kilcommons, Liam, 44
Kim, Eunsol, 27
Kim, Su-In, 34
Kordella, Lee, 24
Kosar, Burcu, 40
Krishnamoorthy, Siddharth, 26

Lamarche, Leslie, 7
Lance, Brandone, 12
Lee, Changsup, 38
Lee, Ji-Hee, 43
Lin, Ting-Han, 23
Lin, YenChieh, 8
Loucks, Diana, 11
Lu, Yang, 36

Maimaiti, Maimaitirebike, 40
Mannucci, Anthony, 17
McGranaghan, Ryan, 14
McTernan, Jesse, 24
Moses, Magdalena, 16

Nossal, Susan, 42

Oscanoa, Julio, 26

Parham, Jonathan, 27
Perlongo, Nicholas, 34
Perry, Gareth, 19
Pilinski, Marcin, 14

Reyes, Pablo, 5
Richmond, Arthur, 4
Riousset, Jeremy, 38
Rojas Villalba, Enrique, 17

Salzano, Michelle, 13
Schroeder, Lynsey, 37
Shen, Yangyang, 29
Shi, Yining, 29
Sivadas, Nithin, 30
Smith, Jonathon, 1
Sousa, Austin, 31
Spann, James, 10
Swboda, John, 18

Troyer, Riley, 40

Vierinen, Juha, 36

Wang, Boyi, 31

Wang, Jun, 19
Wang, Liang, 37
Wu, Jiashu, 32
Wu, Kang-Hung, 22

Yang, Tae-Yong, 7
Yonker, Justin, 43

Young, Matthew, 1

Zhan, Weijia, 12
Zhong, Jiahao, 3
Zhu, Qingyu, 3
Zia, Kenneth, 20
Zou, Ying, 35